

**Universidade de Évora - Escola de Ciências e Tecnologia**

**Mestrado Integrado em Medicina Veterinária**

Dissertação

**Measurement of tissue oxygen saturation during ovariohysterectomy in domestic felines with near-infrared spectroscopy (NIRS)**

Patricia Alexandra Luis Moio

Orientador(es) | David Orlando Ferreira  
Lénio Bruno Martins Ribeiro

Évora 2021

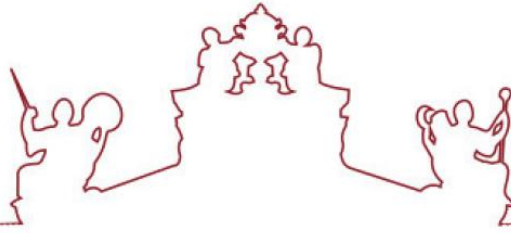
---

---

---

---

---



**Universidade de Évora - Escola de Ciências e Tecnologia**

**Mestrado Integrado em Medicina Veterinária**

Dissertação

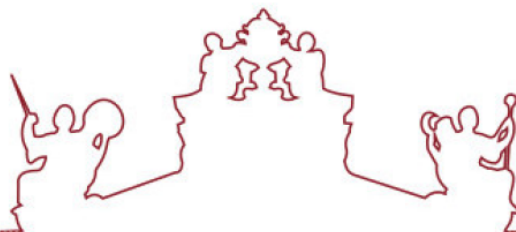
**Measurement of tissue oxygen saturation during  
ovariohysterectomy in domestic felines with near-infrared  
spectroscopy (NIRS)**

Patricia Alexandra Luis Moio

Orientador(es) | David Orlando Ferreira  
Lénio Bruno Martins Ribeiro

Évora 2021





A dissertação foi objeto de apreciação e discussão pública pelo seguinte júri nomeado pelo Diretor da Escola de Ciências e Tecnologia:

Presidente | Rita Payan-Carreira (Universidade de Évora)

Vogais | David Orlando Ferreira (Universidade de Évora) (Orientador)  
Pedro de Pinho e Costa Amorim () (Arguente)

## **Dedications**

First of all, I want to thank my family, especially my parents, my grandmother Adelaide, my aunt Ana and my cousins Andrea and Diogo, since without them my path in veterinary medicine would not have been possible and it would not have been the same. They were always by my side in every moment of my life, including getting my university degree, and gave me strength, motivation and comfort in the most difficult times and when I was exhausted.

I want to give a special thanks to my parents, who taught me to never give up and always do my best, no matter how hard it might be, and to fight for my goals and what I want, and, above all, I want to thank my mother. I do not have enough words to thank her for everything she gave me, especially her patience, support and motivation, and for raising me, alongside my father and family, and for making me the person I am today.

I want to give a big thank you to Professor David Ferreira, for all his patience, motivation, dedication, guidance, and advice and for all the work he has done while I was in my internship and developing my dissertation. Thank you for accepting me and for believing in me and my capabilities, and for having advised me to Centro Hospitalar Veterinário (CHV) and Professor Lénio Ribeiro for my learning during the internship.

I would like to also thank Professor Lénio Ribeiro for accepting to guide this "alentejana", even without any spare time and with a filled schedule, for everything he taught me and for valuing my work.

Moreover, thanks to the wonderful team at Centro Hospitalar Veterinário (CHV), to all the doctors and nurses, for receiving me and teaching me so much, during the almost eight months that we were together, and for all the laughing and companionship. And a special thanks to all my internship colleagues, for their friendship, help, knowledge, and for all the moments of fun and pranks.

I also want to thank Professor Alfredo, for helping me with the statistical analyses in my dissertation.

To Catarina Pereira, from Masimo Corporation Portugal, for helping me with all the information about the device used in my dissertation's study.

Last but not least, I want to thank all my friends for being by my side and supporting me in all moments of my life. The new friends that I made at university and all the old friends that were with me before, either more distant or more present, with better or worse moments, they have always been with me and I know I can always count on them.

## **Measurement of tissue oxygen saturation during ovariohysterectomy in domestic felines with near-infrared spectroscopy (NIRS)**

### **Abstract**

Near-infrared spectroscopy (NIRS) is a noninvasive and continuous technique, easily and quickly to apply, that gives information in real-time of regional tissue oxygen saturation at microcirculation level.

This preliminary study evaluated NIRS technique using the O3™ Regional Oximetry device on sartorius muscle of six female cats, under general anesthesia and submitted to elective ovariohysterectomy.

The tissue oxygen saturation values obtained were  $71.84 \pm 4.85\%$  (65% to 83%). Statistical significance was observed with a positive correlation between NIRS and minimum alveolar concentration, heart rate, and systolic blood pressure, and a negative correlation between NIRS and body temperature. NIRS was not able to detect noxious stimulation.

In conclusion, the normal range of NIRS values in the sartorius muscle in cats under general anaesthesia for elective ovariohysterectomy was  $71.84 \pm 4.85\%$  with cut-off 62%. A question is raised whether NIRS technique can be useful as an indirect indicator of cellular metabolism, taking into consideration the body temperature.

**Keywords:** NIRS; near-infrared spectroscopy; tissue oxygen saturation; sartorius muscle; microcirculation

## **Medição da saturação de oxigénio tecidual durante ovariectomia em felinos domésticos com espectroscopia de infravermelhos próximo (NIRS)**

### **Resumo**

Espectroscopia de infravermelhos próximo (NIRS) é uma técnica contínua e não invasiva, de fácil e rápida aplicação, que fornece informação em tempo real da saturação em oxigénio dos tecidos regionais, a nível da microcirculação.

Este estudo preliminar avaliou a técnica NIRS no músculo sartório de seis gatas, sob anestesia geral, submetidas a ovariectomia eletiva, com o aparelho O3™ Regional Oximetry.

Os valores obtidos de saturação de oxigénio tecidual foram  $71.84 \pm 4.85\%$  (65% to 83%). Identificou-se significância estatística e correlação positiva entre NIRS e concentração mínima alveolar, frequência cardíaca e pressão arterial sistólica, e correlação negativa entre NIRS e temperatura corporal. NIRS não conseguiu detetar estímulos nódicos.

Concluiu-se que os valores de NIRS no músculo sartório em gatas submetidas a ovariectomia sob anestesia geral foi  $71.84 \pm 4.85\%$  com cut-off de 62%. Existe a possibilidade de a técnica NIRS poder ser utilizada como indicador indireto do metabolismo celular, quando correlacionado com a temperatura corporal.

**Palavras-chave:** NIRS; espectroscopia de infravermelhos próximo; saturação de oxigénio tecidual; músculo sartório; microcirculação

“Nothing in life is to be feared, it is only to be understood. Now is the time to understand more, so that we may fear less.”

**Marie Curie**

## Index

I.	Curricular internship.....	1
II.	Introduction .....	2
1.	Tissue oxygenation and perfusion .....	2
1.1.	Monitoring of regional tissue oxygenation and perfusion.....	5
2.	NIRS – Near-infrared spectroscopy.....	7
2.1	Technology.....	8
2.1.1.	NIRS Principles: physics and mathematics bases .....	9
2.1.2.	Near-infrared light and chromophores .....	11
2.1.2.1.	Haemoglobin: Oxyhaemoglobin and Deoxyhaemoglobin .....	13
2.1.2.2.	Cytochrome c-oxidase .....	14
2.2.	Principles related to NIRS spectrometers.....	15
2.3.	NIRS spectrometers .....	16
2.4.	Limitations in near-infrared spectroscopy measurements.....	18
2.5.	NIRS significant value to standard anaesthesia monitoring.....	20
2.6.	Near-infrared spectroscopy monitoring .....	21
2.6.1.	NIRS in skeletal muscle monitoring.....	22
2.6.1.1.	Muscle sites for NIRS measurements in animals .....	24
2.6.1.2.	Normative NIRS values and variability factors .....	26
2.6.2.	Total haemoglobin index .....	26
2.7.	NIRS monitoring in veterinary practice in cats.....	27



III.	Objectives for the study .....	29
IV.	Materials and Method .....	30
V.	Results .....	32
VI.	Discussion.....	36
VII.	Conclusion .....	38
VIII.	Bibliography .....	39

## Index of graphics

- Graphic 1** - Near-infrared spectroscopy (NIRS) absorption spectra of chromophores in equal concentration. (Hb - haemoglobin, HbO<sub>2</sub> - oxyhaemoglobin, Mb - myoglobin, MbO<sub>2</sub> – oxymyoglobin and CtOx - cytochrome c-oxidase (represents the subtraction between the oxidized and the reduced form of cytochrome c-oxidase)). <sup>14</sup>..... 13
- Graphic 2** - Mean values of HR, SBP, MBP, DBP and NIRS from all patients from T0 until the end of sevoflurane administration. (HR- Heart rate; SBP- Systolic blood pressure; MBP- Mean blood pressure; DBP- Diastolic blood pressure; NIRS- Near infrared spectroscopy; rSO<sub>2</sub>- Regional oxygen saturation)..... 32
- Graphic 3** - Mean and standard deviation values of HR, SBP, MBP and DBP from T0 until the end of sevoflurane administration. (HR- Heart rate; SBP- Systolic blood pressure; MBP- Mean blood pressure; DBP- Diastolic blood pressure). ..... 33
- Graphic 4** - Trend of all NIRS (rSO<sub>2</sub>) values from each patient (P) from T0 until the end of sevoflurane administration. (NIRS- Near infrared spectroscopy; rSO<sub>2</sub>- Regional oxygen saturation)..... 33
- Graphic 5** - Boxplot diagram showing median, minimum, and maximum NIRS (rSO<sub>2</sub>) values from each patient from T0 until the end of sevoflurane administration. (NIRS- Near infrared spectroscopy; rSO<sub>2</sub>- Regional oxygen saturation). ..... 34
- Graphic 6** - Noxious stimuli and the respective NIRS (rSO<sub>2</sub>) values along the sequential surgical events during the anaesthetic procedure. Data are mean ± standard deviation. (T0- five minutes after tracheal intubation; TC- Surgical towel clam; SkI- Skin incision; LAI- Linea alba incision; LSLR- Left suspensory ligament rupture; LPL- Left pedicle ligature; RSLR- Right suspensory ligament rupture; RPL- Right pedicle ligature; UT- Uterine body traction; UBL- Uterine body ligature; UBT- Uterine body transection; CLA- Closure of the linea alba; ECLA- End closing linea alba; SkC- Skin closure; ESKC- End of skin closure; NIRS- Near infrared spectroscopy; rSO<sub>2</sub>- Regional oxygen saturation). ..... 34
- Graphic 7** - Mean values of NIRS and body temperature from all patients, during the study period. (NIRS- Near infrared spectroscopy; rSO<sub>2</sub>- Regional oxygen saturation; T- Body temperature).35

**Index of tables**

**Table 1-** Pearson's ( $\rho$ ) correlation coefficient and p-values between Near-infrared spectroscopy (NIRS) and sevoflurane minimum alveolar concentration (MAC), body temperature (Temp), heart rate (HR), systolic blood pressure (SBP), diastolic blood pressure (DBP) and mean blood pressure (MBP). ..... 35

## Index of figures

<b>Figure 1</b> - Physiologic, pathologic and therapeutic factors that can influence the value of central venous oxygen saturation. <sup>12</sup> .....	3
<b>Figure 2</b> - Uptake and delivery of oxygen in the organism to tissues. ( $O_2$ – oxygen, $DO_2$ – oxygen delivery, $O_2ER$ – oxygen extraction, $VO_2$ – oxygen utilization, $CO$ – cardiac output, $ABP$ – blood pressure, $SVR$ – vascular resistance, $PvO_2$ – mixed venous oxygen pressure, $CvO_2$ – mixed venous blood oxygen content, $PaO_2$ – arterial oxygen partial pressure, $CaO_2$ – arterial blood oxygen content, $PtO_2$ – local tissue oxygen, $Hg$ – quantity of patient’s haemoglobin, %SatHB – saturation of haemoglobin with oxygen). <sup>17</sup> .....	4
<b>Figure 3</b> – Techniques and summary of their clinical applications for monitoring regional perfusion through microcirculation, extracellular space or mitochondrial. (LDF - Laser Doppler flowmetry; MRS - Magnetic Resonance Spectroscopy; NIRS - Near-infrared Resonance Spectroscopy; $O_2$ - Oxygen; SDF - Sidestream Dark Field; $tPO_2$ - Tissue Oxygen Tension). <sup>10</sup> .....	7
<b>Figure 4</b> - Representation of near-infrared spectroscopy (NIRS) and the main chromophores’ location in muscle tissue. ( $HbO_2$ – oxyhaemoglobin; $Hb$ – deoxyhaemoglobin; $MbO_2$ - oxygenated myoglobin; $O_2$ – oxygen; $H^+$ - hydrogen; $H_2O$ - water). <sup>14</sup> .....	12
<b>Figure 5</b> - Technical details of tissue oximetry with near-infrared spectroscopy (NIRS) in reflectance mode: pathlength of near-infrared light, when emitted and received by the optodes of NIRS probe, in tissue bed (the size of the cross-section area of each different vessels depends of blood flow velocity, where capillary is the largest because is the slowest) and light travelling (line 1 and 2 - absorbed by haemoglobin, line 3 and 4 – absorbed by other existing chromophores, line 5 – received by deep detector, line 6 – received by shallow detector, line 7 – light lost). <sup>72</sup> . 15	15
<b>Figure 6</b> – Absorption spectra, in logarithm base, for the different chromophores present in biologic tissue that can influence Near-infrared spectroscopy measurements, with the representation of the “optical window” to use in this monitoring.( $O_2Hb$ – oxyhaemoglobin, HHb - deoxyhaemoglobin, CtOx - cytochrome c-oxidase). <sup>1</sup> .....	18
<b>Figure 7</b> - Representative values of oxygen saturation in different tissues in a dog model, where the arterial values are identified through dotted lines and the venous values by solid black line. <sup>105</sup> .....	21
<b>Figure 8</b> - Representation of skeletal muscle oxygen saturation measurement with near-infrared spectrophotometry, placed above the tissue bed. <sup>121</sup> .....	23

**Figure 9** - NIRS (near-infrared spectroscopy) sensors placed over the sartorius muscles of a dog, using two different NIRS devices: INVOS™ (right leg) and Inspectra™ (left leg).<sup>124</sup> ..... 24

**Figure 10** - Scheme of sartorius muscle with its arterial supply in canine topographic anatomy. Adapted from<sup>125</sup> ..... 25

**Figure 11** - O3™ Regional Oximetry® device (Masimo Corporation, Irvine, CA, USA), Mindray BeneView T8 monitor and mechanical ventilator Mindray WATO EX-20 Vet (Mindray Medical International Co., Ltd., Shenzhen, China) used for this study at the Centro Hospitalar Veterinário. (Picture by Patrícia Moio) ..... 31

## List of abbreviations

**CNS** - Central nervous system

**CO** - Carbon monoxide

**CO<sub>2</sub>** - Carbon Dioxide

**CW** – Continuous wave

**DBP** – Diastolic blood pressure

**EtCO<sub>2</sub>** – End-tidal carbon dioxide

**FD** – Frequency domain

**H<sub>2</sub>O** - Water

**H<sub>2</sub>S** - Hydrogen sulfide

**HNO** - Nitroxyl

**HR** – Heart rate

**LED** – Light-emitting diode

**MAC** – Minimum alveolar concentration

**MBP** – Mean blood pressure

**NIR** – Near-infrared radiation

**NIRS** – Near-infrared spectroscopy

**NO** - Nitric oxide

**NO<sub>2</sub><sup>-</sup>** - Nitrite

**O<sub>2</sub>** - Oxygen

**PaO<sub>2</sub>** – Partial pressure of oxygen

**PCO<sub>2</sub>** - Partial pressure of carbon dioxide

**rSO<sub>2</sub>** – Regional oxygen saturation

**SaO<sub>2</sub>** – Haemoglobin oxygen saturation

**SBP** – Systolic blood pressure

**SPO<sub>2</sub>** – Peripheral oxygen saturation

**StO<sub>2</sub>** – Tissue oxygen saturation

**TCSPC** – Timed-correlated single photon counting

**TD** – Time domain

**THI** – Total haemoglobin index

**TOI** – Tissue oxygen index

## **I. Curricular internship**

The internship was performed at Centro Hospitalar Veterinário (CHV), in the city of Porto, from September 2019 to February 2020.

This veterinary referral hospital offers a rotating internship program, where interns pass through the different specialized services and work with the clinical team under their supervision. The duration of the daily shifts was eight hours during the weekdays, eight or twelve hours one weekend day, or night shift and staff holidays. The clinical areas of rotation were surgery, diagnostic imaging, medical consultation and hospitalization.

During the service in surgery department, the interns helped to prepare the patient, participated in anaesthetic procedures and monitoring, assist the surgeon during soft tissues and orthopaedic surgeries, and learn about the preparation procedures of surgery room, asepsis protocols, dressing for surgery, correct way to deliver the surgical instruments and to clean them after surgical interventions.

In the imaging department, the interns had the opportunity for helping in patient's preparation, restraining and anaesthetic monitoring, participating and discussing the results of ultrasound and computed tomography exams, echocardiography exams, and endoscopy procedures.

During medical consultation, the interns accompany the doctors along the different consults and are included in clinical case and patients historical. The medical areas accompanied during medical consults were internal medicine, preventive medicine, and consultations on specialises areas such as neurology, dermatology, orthopaedics, cardiology, oncology, and nutrition. During the consults, the intern followed patient's physical exam, clinical exams, diagnose, and clinical decisions.

In the hospitalization service, the interns participated in the examination and treatments (preparation and administration) until the feeding, walks and physiotherapy, with the guidance and supervision of doctors and nurses, of the hospitalized animals. Additionally, the intern had the opportunity to participate in the clinical procedures, patient's monitorization, laboratory analyses, blood transfusions, patient's recovery and assist in emergency and critical care cases.

During the internship I also had the opportunity to public present and discuss scientific articles, attend to lectures organized by the senior doctors, and participate in research projects.

## II. Introduction

The possibility of transmitting continuous light through human tissues is being investigated since the 19<sup>th</sup> century.<sup>1</sup> An important step towards the development of near-infrared spectroscopy (NIRS) potential was, in 1938, the demonstration for the first time, of the possibility to measure oxyhaemoglobin and deoxyhaemoglobin in human tissue, using two wavelengths (red and infrared light).<sup>2</sup> referred by 1.<sup>3</sup> Another important step that contributed for the evolution of NIRS technology, was the development of its ability to perform quantitative measurements, based on the Beer-Lambert law, discovered in 1729 by the mathematician Bouguer.<sup>4</sup> referred by 1 Over the years, the application of this law to NIRS development led to the possibility of quantifying concentrations in 1852,<sup>5</sup> but it was only valid in non-scattering media.<sup>1</sup> As the biological tissues are considered scattering media, the use of NIRS technology in biological tissues with Beer-Lambert law was still not very accurate and could not be applied.<sup>1</sup> The development of the Modified Beer-Lambert law, by Delpy in 1988,<sup>6</sup> an extension of Beer-Lambert law that includes scattering light loss intensity, became the basis for NIRS technology.<sup>1</sup> Over the last 40 years, NIRS technology has been progressively investigated, integrated and approved in several systems for clinical use, also being tested and applied in many different areas.<sup>3</sup>

### 1. Tissue oxygenation and perfusion

Oxygen (O<sub>2</sub>) delivery is maintained by an adequate cardiac output, intravascular volume, systemic blood pressure and an adequate vascular resistance, which clearly show the importance of blood flow and of the geometrical structure organization of blood vessels on patients monitoring.<sup>7,8</sup>

Cells need energy for their functions and for maintaining homeostasis.<sup>9</sup> Thus, it is essential a functional blood circulatory system to transport all the necessary nutrients, O<sub>2</sub> and other essential molecules (figure 1).<sup>8,10</sup> During anaesthesia, surgery and intensive care procedures, sudden physiologic changes can compromise homeostasis, and patients' monitoring is crucial to address these changes as early as possible, towards restoring normal function and, consequently, decrease patients' morbidity and mortality.<sup>11</sup>



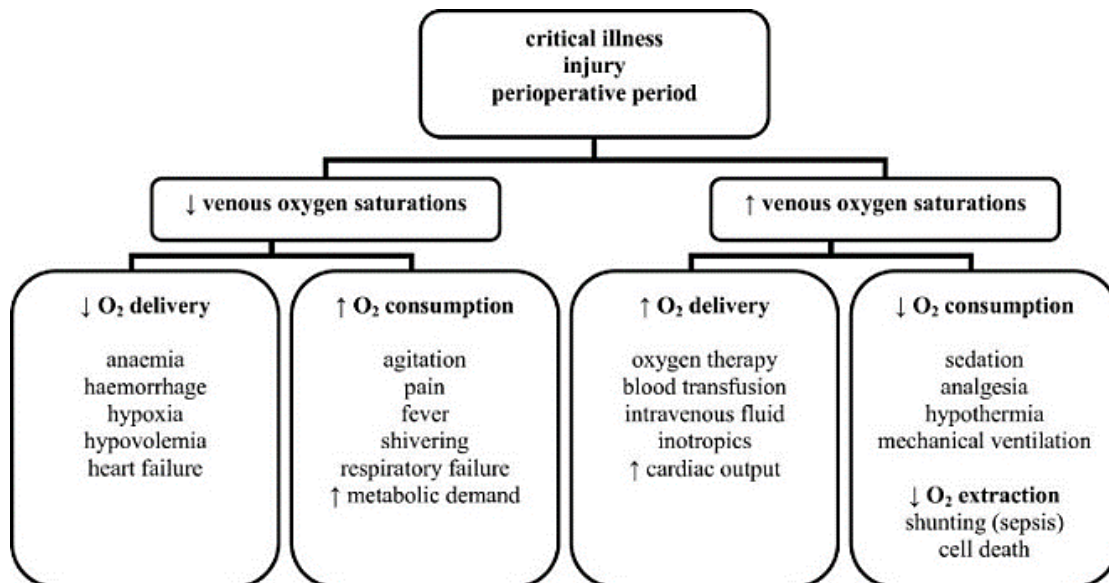


**Figure 1** - Physiologic, pathologic and therapeutic factors that can influence the value of central venous oxygen saturation.<sup>12</sup>

Maintaining haemodynamic stability is the primary goal during patients' monitoring, towards preserving an adequate delivery of O<sub>2</sub> and other nutrients, and remove products resulting from cell metabolism.<sup>3,7,10</sup> If haemodynamic stability fails, it will cause tissue hypoperfusion and consequent organ dysfunction or failure.<sup>10</sup> Ultimately, haemodynamic shock can occur and may lead to multiorgan failure.<sup>12-14</sup>

Local O<sub>2</sub> deficits may pass unnoticed, and only be identified later when the functional tissue is already damaged.<sup>3</sup> There is a narrow window of opportunity to compensate the deficits and, if enough oxygen is provided to restore cellular tissues metabolism, it is possible to prevent the occurrence of secondary events and the progress to organs dysfunction.<sup>10,14</sup> Evaluating the global oxygenation status of tissues, which include the measurement of cellular O<sub>2</sub> supply (to identify occult and initial hypoxia events) and O<sub>2</sub> consumption (dysoxia events), is important to compensate the physiological imbalances as early as possible.<sup>3,7,10</sup>

In the last decade, studies have shown that macroperfusion is important in a general plan of controlling the cardiovascular function but, relatively to the end-organ tissue oxygenation, it does not provide early detailed information, being these macrocirculatory parameters directed to patient's central haemodynamic status.<sup>11</sup> Studies based in the pathophysiology of organ failure, and in the perfusion and tissue oxygenation, showed that monitoring microcirculatory system is more accurate than monitoring macrocirculatory system in identifying regional tissue hypoxia and hypoperfusion.<sup>7</sup>

The microvasculature includes all the vessels with a diameter below 100µm (arterioles, venules and capillaries).<sup>10,15</sup> This microvessels network is essential to supply regional tissues with enough O<sub>2</sub> and nutrients for their metabolism. Due to its geometrical structure and organization, there is a certain heterogeneity among microvessels, but some biological mechanisms (angiogenesis, blood flow regulation, and others) allow to balance the distribution of hematocrit, blood flow, blood velocity, blood pressure, and adapting the blood vessels' wall shear stress to allow more efficient nutrient and gas exchanges between tissues and the circulatory system (figure 2).<sup>8,16</sup>

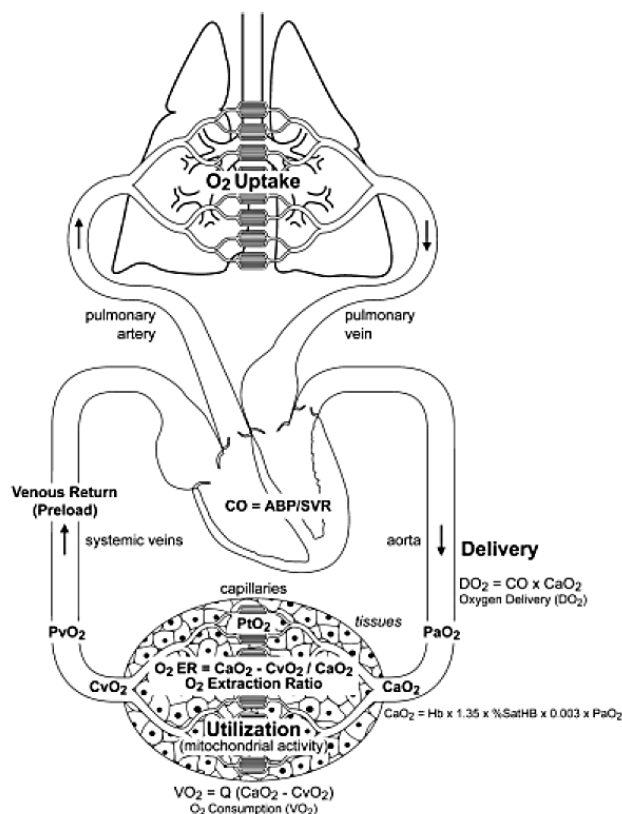


**Figure 2** - Uptake and delivery of oxygen in the organism to tissues. (O<sub>2</sub> – oxygen, DO<sub>2</sub> – oxygen delivery, O<sub>2</sub>ER – oxygen extraction, VO<sub>2</sub> – oxygen utilization, CO – cardiac output, ABP – blood pressure, SVR – vascular resistance, PvO<sub>2</sub> – mixed venous oxygen pressure, CvO<sub>2</sub> – mixed venous blood oxygen content, PaO<sub>2</sub> – arterial oxygen partial pressure, CaO<sub>2</sub> – arterial blood oxygen content, PtO<sub>2</sub> – local tissue oxygen, Hg – quantity of patient's haemoglobin, %SatHB – saturation of haemoglobin with oxygen).<sup>17</sup>

Microcirculation includes more than 60% of the overall peripheral resistance of the circulatory system, being the main network responsible for maintaining the balance between blood pressure and the organs' tissues blood supply.<sup>18</sup> The size of vascular bed, the number of vessels per tissue area, and the blood flow per mass of tissue, are different between organs. Thus, significant changes in the blood pressure will individually affect each organ and, consequently, determine the severity of the lesions.<sup>19</sup>

The main function of the microcirculation is providing an efficient interface between the blood components and local tissue perfusion, accordingly to every tissue's metabolic needs.<sup>20</sup> Tissue perfusion is regulated by the Central Nervous System (CNS) but can be influenced by

pain, stress, hypothermia and systemic inflammatory response, which can cause and potentiate blood flow maldistribution within the vessels bed.<sup>17</sup> Endothelial glycocalyx, a layer lining the vascular endothelium, and composed by soluble plasma components, proteoglycans and glycosaminoglycans that separate endothelial cells from blood stream, is also an influencing factor to consider in microcirculation perfusion.<sup>20,21</sup> The glycocalyx has a thromboresistant nature due the presence of anticoagulant molecules, and its main role is to protect the blood vessels dynamics. By controlling vascular permeability, restricting blood-vessel's wall interaction (red cells, platelets and white cells), adjusting the resistance to shear stress forces, and by enabling balanced signalling, and modulating inflammatory responses, blood viscosity and hematocrit inside the microvasculature, the glycocalyx assures the maintenance of an ideal blood-body tissues interface. When the glycocalyx barrier is damaged, it may lead to tissue oedema formation and decreased microvasculature perfusion.<sup>21</sup>

Thus, monitoring and evaluating the microvasculature is an important parameter during anaesthetic procedures and critical care monitorization, and must always be associated with the monitoring of macrocirculatory parameters.<sup>7</sup>

### **1.1. Monitoring of regional tissue oxygenation and perfusion**

Cardiorespiratory system has an important role in providing enough O<sub>2</sub> for cells functions and tissues survival. The gas exchanges and normal blood flow in the microcirculatory system is essential for an effective O<sub>2</sub> delivery to the biological tissues.<sup>20,22</sup> In order to assure an efficient blood gases transportation to and from the tissues, it is essential to having intact and normal function of respiratory mechanics and air-blood-barrier in the lungs, intact macrohaemodynamic, normal values of haemoglobin levels, and a functional microcirculatory blood flow.<sup>20</sup> Thus, a preoxygenation with O<sub>2</sub> during preanesthetic/induction sequence is recommended for providing an adequate O<sub>2</sub> saturation of haemoglobin.<sup>23</sup>

The balance between ventilation and perfusion is important to prevent hypoxemia, because any imbalance will change the carbon dioxide (CO<sub>2</sub>) and O<sub>2</sub> blood levels, and may result in tissues hypoxia.<sup>22</sup> If ventilation decreases relatively to the blood perfusion pressure, the CO<sub>2</sub> alveolar concentration will increase, and the O<sub>2</sub> blood concentrations will decrease. The O<sub>2</sub> alveolar pressure is not sufficient to assure a normal CO<sub>2</sub>/O<sub>2</sub> exchange, and the increased CO<sub>2</sub> blood pressure will promote a rapid blood/alveoli CO<sub>2</sub> passage.<sup>24</sup>

On the contrary, if the blood perfusion pressure decreases relatively to the ventilation pressure, the CO<sub>2</sub> alveolar concentrations will decrease due to the perialveolar capillary hypotension/hypoperfusion, which will compromise the passage of CO<sub>2</sub> from the blood to the alveoli. Also, an increase in the O<sub>2</sub> alveolar concentrations will occur due to decreased blood perfusion pressure that will negatively influence the O<sub>2</sub> crossing of the alveolar-blood barrier.<sup>24</sup>

The pressure of CO<sub>2</sub> and O<sub>2</sub> in the blood condition the sympathetic outflow and the vascular tonus, and small changes in the vasculature diameter may compromise tissue perfusion and blood pressure.<sup>25</sup> Although significant changes in the pressure of CO<sub>2</sub> and O<sub>2</sub> in the blood can quickly be reversed, the effect of these changes in the vascular bed extend beyond the normalization of the blood O<sub>2</sub> and CO<sub>2</sub> pressures.<sup>26</sup> Thus, both O<sub>2</sub> and CO<sub>2</sub> blood pressures should be carefully monitored.

Mechanical ventilation allows us to adjust the ventilation parameters to achieve normal physiological blood gases concentrations, even in patients with pathological conditions such as alveolus collapse, atelectasis, acute respiratory distress syndrome. Additionally, mechanical ventilation allows alveolar recruitment manoeuvres, which optimizes alveolar gas exchange, and, also, relieves respiratory musculature, which decreases the O<sub>2</sub> consumption by the respiratory muscles increasing the circulating concentrations of nutrients and O<sub>2</sub> available to supply other organs.<sup>27,28</sup>

Mechanical ventilation is based on a positive-pressure ventilation, which is the contrary of voluntary breathing, where exists a negative-pressure force to get air into the lungs. Pulmonary volume controls and influence intrathoracic pressure and pulmonary circulation vasculature, while intrathoracic pressure is responsible for influencing the systemic circulation and may cause profound alterations at this level. When using mechanical ventilation, it is important to be aware of significant haemodynamic changes that may occur as a consequence of using this ventilatory technique: (i) alterations on the right and left ventricular ejection and loading; (ii) decrease of venous return when associated with hypovolemia, or right atrial pressure increase due to intrathoracic pressure increase (intra-abdominal pressure increasing due to diaphragmatic descent also influence the venous return, but lesser than these two previous factors); (iii) similarities to cardiac tamponade when high lung volume compresses the heart; (iv) alterations of autonomic tone due to lung volume changes; (v) increasing lung volume leads to a correspondent increase in the pressure difference between airways and pleura and, when it exceeds the pulmonary artery blood pressure, pulmonary vascular resistance increase due to the collapse of blood vessels passing into the alveolar space, and (vi) decrease of end-expiratory lung volume leading to alveolar collapse, which induce an increase in the pulmonary vasomotor tone due to the hypoxic pulmonary vasoconstriction.<sup>22,27,28</sup>

The traditional methods used to monitor tissues perfusion include physical examination (heart rate, pulse quality, mucous membrane colour and capillary refill time), body temperature, mental status, arterial blood pressure, central venous pressure and urine output.<sup>7,10,12,14</sup> Physiologic markers (lactate concentration level, acid-base status and central/mixed venous oxygen saturation) and the implementation of techniques, such as pulse oximetry, blood gas analyses and pulmonary arterial or central venous catheterization, also help to measure globally

tissue perfusion and oxygenation.<sup>7,12,29,30</sup> However, they do not express the regional differences and difficult the early detection of local hypoxia and dysoxia events.<sup>10,30,31</sup>

Currently, some new methods are being used to monitor regional perfusion (via microcirculation, mitochondrial or extracellular space), providing a non-invasive or minimally invasive monitorization (figure 3).<sup>7,10,31</sup>

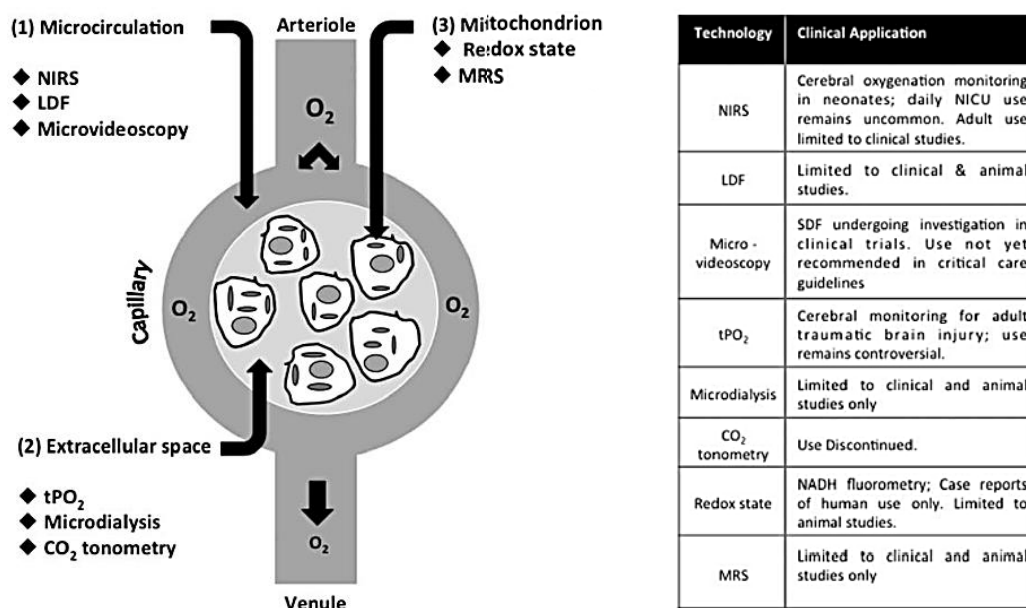


**Figure 3** – Techniques and summary of their clinical applications for monitoring regional perfusion through microcirculation, extracellular space or mitochondrial. (LDF - Laser Doppler flowmetry; MRS - Magnetic Resonance Spectroscopy; NIRS - Near-infrared Resonance Spectroscopy; O<sub>2</sub> - Oxygen; SDF - Sidestream Dark Field; tPO<sub>2</sub> - Tissue Oxygen Tension).<sup>10</sup>

The gold standard for monitoring microvascular perfusion are the microvideoscopic techniques.<sup>16</sup> Vasoreactivity testes such as laser doppler and near infrared spectroscopy (NIRS), gastric tonometry, sublingual capnometry, transcutaneous CO<sub>2</sub> measurements, contrast-enhanced ultrasounds, glycocalyx biomarkers and venoarterial PCO<sub>2</sub> (partial pressure of CO<sub>2</sub>) gradients are other methods available for monitoring microvascular compartment.<sup>7,16</sup>

## 2. NIRS - Near-infrared spectroscopy

The absorption spectrums of oxyhaemoglobin and deoxyhaemoglobin were described in 1862 by Hoppe-Seyler<sup>32</sup>, and in 1864 by Stokes<sup>32</sup>, respectively, showing the importance of haemoglobin as an O<sub>2</sub> transporter and for monitoring oxygenation.<sup>1</sup> The study that records the first attempt to monitor tissue oxygenation, in a non-invasive way, dates to 1876, when von Vierordt study a decrease of red-light transmission through a human hand, when an ischemic process occurred.<sup>33</sup> referred by<sup>1,3,34</sup> In 1894 Hüfner<sup>35</sup> was able to measure the absolute and relative

amount of oxyhaemoglobin and deoxyhaemoglobin in in vitro studies using spectroscopy.<sup>1</sup> Nevertheless, the studies on spectroscopic analyses of tissue oxygenation were only continued some decades later (1930s).<sup>1,3</sup> Matthes and Gross, in 1939, published a study alerting for a variation of red and infrared transmission accordingly with the amount of blood oxygenation.<sup>36</sup> referred by <sup>3</sup> Jobsis, in 1977,<sup>37</sup> was the first researcher to investigate and describe the applications of NIRS as a method for measuring the O<sub>2</sub> metabolic state in the brain. He used a cat's head to radiate with near-infrared light and, with continuous measurements, proved that there is a variation in the intensity of the transmitted light based on the level of oxygenation in the brain tissue.<sup>3,15</sup>

Initially, NIRS was used in paediatric, cardiac and neuroanesthesia service but the technique was later discredited due to some studies that demonstrated the possibility of false positives and negatives readings, and anecdotal papers<sup>38,39</sup> that question the validity of NIRS monitoring. However, with a deeper understanding of NIRS characteristics and limitations, it was possible to understand that all the NIRS observations published in these studies are possible to occur, but they do not invalidate the use of NIRS to monitor tissue oxygenation.<sup>3</sup> With the evolution of knowledge and technological development, NIRS monitoring has become more accepted for assessing tissue oxygenation over the last 40 years. In the 1990's NIRS technology started to be commercialized and used in clinical practice, to provide real-time continuous tissue O<sub>2</sub> saturation measurements in brain and somatic tissue. In the last years, the interest in using NIRS for assessing tissue oxygenation under general anaesthesia has increased significantly, and this technology is licensed worldwide for using in clinical setups.<sup>3,15</sup>

## **2.1. Technology**

The development of diffuse optical methods, which is a technology based on absorption and scattering properties of near-infrared light, allowed to acquire important information for patients monitoring, specially about brain activity. The general concept, of techniques that integrate this group, is to apply near-infrared light in a tissue and use the absorption spectra for this radiation of absorbent molecules (chromophores), which are present in the tissue, to interpret the emerging light levels detected as changes of chromophores concentrations. It can be named by near-infrared spectroscopy, diffuse optical tomography and/or near-infrared imaging, and the diffuse optical techniques are considered excellent in temporal sensitivity and reasonable in spatial sensitivity.<sup>40</sup>

Near-infrared spectroscopy (NIRS) is a continuous, real-time and noninvasive technique used to monitor oxygenation, haemodynamic and metabolism of tissues, and it has proven to be an early indicator of organ ischaemia and oxygenation changes, when compared to other methods such as pulse oximetry, lactate, mental status, blood pressure and others.<sup>31</sup> The NIRS

technique allows to monitor the nonpulsatile environment, including the local microvasculature, intracellular space and low-pressure areas, making it possible to measure the tissue O<sub>2</sub> saturation in the end point of the O<sub>2</sub> delivery.<sup>31,41,42</sup>

### **2.1.1. NIRS Principles: physics and mathematics bases**

NIRS is a transillumination spectroscopy technology that uses near-infrared light, a wavelength of 700-1000nm from the electromagnetic spectrum. The photons transmitted by the laser, at these wavelengths, have the capacity to pass through several centimetres of different types of tissues (including bone), and reach deeper structures without great light attenuation, due to the low capacity of infrared light to be absorbed by the tissues.<sup>7,30,31,42-44</sup> The fundamentals for this technique are based in physics principles, but also involve knowledge in the fields of biochemistry and mathematics.

Each substance has a unique and characteristic spectrum of absorption and optical properties when irradiated (scattering and absorption coefficient, that are wavelength dependent), which allow to identify and determine the concentration of each component.<sup>42,45,46</sup> Biological molecules can change their optical properties due to chemical or bonding reactions, and one example is the oxygenation and deoxygenation of haemoglobin that change its absorption spectrum in each of its forms<sup>30,41</sup> (oxyhaemoglobin absorbs more infrared wavelength, closer to 800-1000nm, than deoxyhaemoglobin, which absorbs more closer to 600-800nm).<sup>7</sup> The absorption spectrum is an important measurement tool to evaluate the optical properties of substances. It provides quantitative information, such as concentration, biological activities and the shape or size of suspended particles.<sup>47</sup>

Other principles that theoretically support NIRS technology, is that biological tissues react differently to each wavelength of light and are relatively transparent to some of them, like red and infrared radiation.<sup>42,48</sup> When the light beam is transmitted and transverse the substances, like tissue or blood, the reaching surface of each substance will absorb, reflect, or scatter that light in different degrees and intensity.<sup>7,14,31</sup> Depending on each component, their chemical transformations over the time and the photons emitted, the propagation of each wavelength light in the tissues will be different.<sup>42</sup> The transmission of light through reflection depends on the angle of the irradiated light beam and the tissue surface, while absorption and scatter depend on the wavelength, the molecules properties of substance and the size and measurement geometry of each type of tissue, with an indirect proportion between scattering and the increase of wavelength.<sup>7,42,48</sup>

The NIRS sensors' optical spectrometers have photodetectors that are used to collect and measure the intensity of the emerging light that was not absorbed and returned to the tissue surface. The amount of light detected is less than the transmitted and, through mathematic

calculations, as referred above, it is possible to perform a quantitative and qualitative analysis of the tissue oxygenation.<sup>14,15,30,42,43,49</sup>

NIRS data quantification is difficult to perform in biologic tissues because these are considered a scattering medium, which is responsible for changing the optical path length of some wavelength, especially near-infrared. This problem of NIRS quantification in biological tissues also depends on other factors: (i) the light absorption is dependent of the components and chromophores existing within the tissue (different spectrum of absorption and concentrations of each component), (ii) the light scattering, (iii) tissues type, size and measurements geometry, and (iv) tissue absorption and scattering coefficients. These factors lead to light attenuation and make it impossible to know the absolute value of light lost and, consequently, the true absorption value, which influences the calculation results of the concentration of the absorbers.<sup>7,50,51</sup>

Scattering is responsible for the loss of approximately 80% of the infrared light intensity emitted, making scattering the most important parameter responsible for light attenuation, and a significant issue that is still continuously being addressed in improving NIRS technology. The refractive index induce this effect of scattering, and its variation is related to the cells constituents, and the relationship between and within cells environment.<sup>7,42</sup> This index can be a useful tool in large tissues, where the transillumination technique is difficult to apply (brain, for example). In this situation, when the light enters the tissue it's scattered and transmitted through all the matter, due to the diffuse photon density and the different tissues layers, and the emerging light that returns to the surface and it's detected by NIRS, gives essential information about a bigger sample of that large tissue.<sup>50-52</sup>

NIRS technology is based in the Beer-Lambert law to provide the physical and mathematical basis for the O<sub>2</sub> tissue calculations. In spectroscopy, this law is commonly used to measure the light absorbance and analyse the transmission of light through solutions, which states that transmission is a logarithmic function that relates density/concentration of the absorbers. This law neglects light scattering and assumes that variation of light attenuation is only influenced by absorption changes. Also, it defends a direct and proportional relationship between the quantity of light absorbed by a substance and its absorption coefficient at a specific wavelength, the concentration of the substance and the path length of photons.<sup>3,15,42,53,54</sup>

Nevertheless, biologic tissues are frequently assumed as an optical homogeneous substance to simplify the mathematical calculations for haemodynamic monitoring. But, in fact, it is a scattering medium composed of many different layers and compartments with different optical properties and scattering coefficients, depending on the tissues adipose tissue, bone and vasculature.<sup>53</sup> To overcome the scattering in biologic tissues, it was introduced the Modified Beer-Lambert law in NIRS calculations, that defends a non-linear relationship as it depends on



both scattering and absorption coefficients. It takes into account the scattering light, and relates differential changes in the optical density with those that occur in the absorption coefficient.<sup>50,53-55</sup> To obtain a natural and proportional constant between the measured intensity and the sample's absorption light, the mean of the photon path length during its transmission in a highly scattering tissue is used to better estimate the photons path length and provides this constant. Since attenuation of light depends on absorption and scattering, and the light scatter has a significant importance on the biologic tissues and in the emitted light intensity, it is crucial to consider this phenomenon of light lost to accurately estimate the true tissue light absorption value, and the quantitative data from regional O<sub>2</sub> saturation.<sup>7,15,53,54</sup>

However, the efficiency of the Modified Beer-Lambert law analysis may produce some inaccurate quantification, because of the uncontrolled changes in differential pathlength factor due to the initial alterations of source-detector positions and, consequently, its distance, and the optical properties of the irradiated tissue.<sup>55</sup> To simplify and improve the accuracy of the pathlength measurement, new algorithms, mathematical functions, models and techniques (Spatially resolved spectroscopy<sup>56-58</sup> and Generalized Beer-Lambert model, using Lambert-W function<sup>55</sup>, for example) have been developed and tested to decrease the influence of wave-dependent pathlength in absorption calculations, and to improve NIRS values accuracy when used in biological environments.<sup>14,51,52,55</sup>

### **2.1.2. Near-infrared light and chromophores**

Near-infrared radiation (NIR) is used in NIRS technology and it's a subdivision of infrared light, being the closest region to the visual spectrum (radiation detectable by the human eye).<sup>44</sup> Each substance have different indices of reflection, absorption and refraction, and consequently different scattering effect, which will influence the transmission and penetration of light through the substances. NIR is characterized by having low scattering and absorption effect in biological tissues, which gives it the ability to pass through different type of tissues and penetrate deep layers, reaching brain cortex, skeletal muscle tissue and, also, organs tissues.<sup>30,34,40</sup> But, due to the optical properties of water and to the scattering and absorption effect variability between the different biological components, it is important to use a NIR wavelength range that will allow a deep optical penetration and collecting the information of interest.<sup>34,45</sup> The "optical window" (the wavelength range of near-infrared light that is less absorbed and allows to pass through the different tissue layers with almost no absorption) is 650-950 nm,<sup>40</sup> and NIRS measurements usually use a wavelength range of 700-850nm.<sup>34</sup> At this range, the light penetration into tissues is not limited by the water and lipid components, and can reach higher tissue depths.<sup>34</sup>

The biologic tissues contain light absorbing molecules of near-infrared light, called chromophores, that contribute to light attenuation (figure 4).<sup>59</sup>

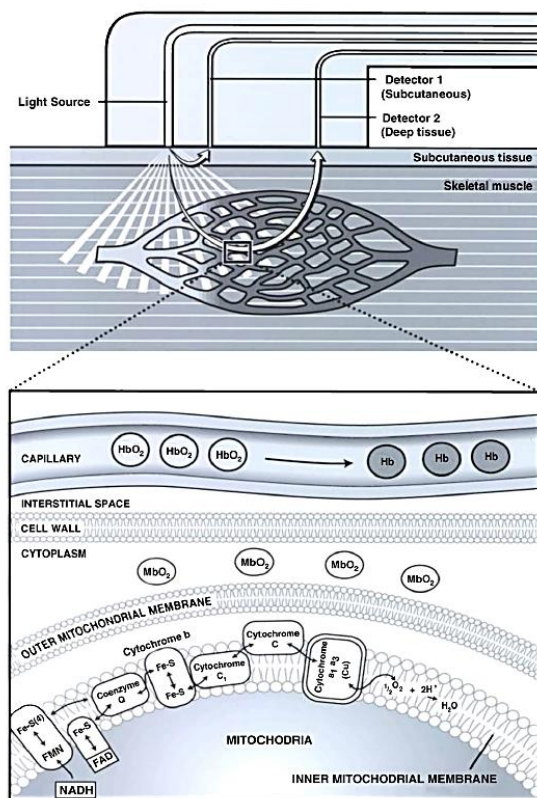
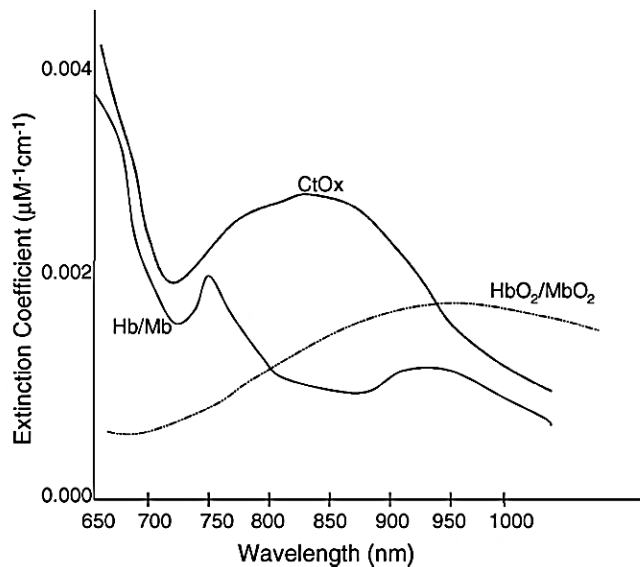


**Figure 4** - Representation of near-infrared spectroscopy (NIRS) and the main chromophores' location in muscle tissue. (HbO<sub>2</sub> – oxyhaemoglobin; Hb – deoxyhaemoglobin; MbO<sub>2</sub> - oxygenated myoglobin; O<sub>2</sub> – oxygen; H<sup>+</sup> - hydrogen; H<sub>2</sub>O - water).<sup>14</sup>

When the transparency of the biological tissue is related to the absorption capacity of the existing chromophores at this wavelength range, it becomes possible to measure haemodynamic variations, metabolic activity and determine the concentration of this molecules by calculating the attenuated light levels.<sup>59</sup> The existence of different absorption spectra allows to separate and distinguish each chromophore in NIR range with spectroscopy technique. The chromophores of biological interest for haemodynamic monitoring are the O<sub>2</sub>-dependent chromophores, and NIRS measurements depend on the absorption changes caused by their connection with the O<sub>2</sub> molecules.<sup>15</sup> These molecules are haemoglobin (oxyhaemoglobin, deoxyhaemoglobin and total haemoglobin, that are measured by NIRS),<sup>15,31,34,48</sup> cytochrome c-oxidase and myoglobin.<sup>7,10,15,31</sup> In NIRS technology, light attenuation and the calculation of tissue O<sub>2</sub> saturation are mainly based on the contribution of oxy- and deoxyhaemoglobin, while myoglobin and cytochrome c-oxidase have a smaller contribution because of their low concentrations when comparing to haemoglobin concentrations.<sup>7,10,31,48</sup>

In graphic 1 is represented the extinction coefficient, at each wavelength of near-infrared range, of the principal chromophores. The extinction coefficient represents the absorbing force of each molecule at a particular wavelength.<sup>48</sup>



**Graphic 1** - Near-infrared spectroscopy (NIRS) absorption spectra of chromophores in equal concentration. (Hb - haemoglobin, HbO<sub>2</sub> - oxyhaemoglobin, Mb - myoglobin, MbO<sub>2</sub> - oxymyoglobin and CtOx - cytochrome c-oxidase (represents the subtraction between the oxidized and the reduced form of cytochrome c-oxidase)).<sup>14</sup>

### 2.1.2.1. Haemoglobin: Oxyhaemoglobin and Deoxyhaemoglobin

Haemoglobin is an ubiquitous iron-containing metalloprotein that is present within the erythrocytes and is responsible for the transport of O<sub>2</sub> from the lungs to the diverse tissues for assuring aerobic cellular metabolism. The red blood cell is important to provide a microenvironment that provide the necessary conditions for the modulation of haemoglobin and to optimize the binding and transport of O<sub>2</sub>. In mammals, this molecule is a tetrameric protein formed by four chains, two α-subunits and two β-subunits, and each one has a haem group, which is an amphipathic molecule with the hydrophobic part attached to the inside of the globin and the polar part on the surface. In the center of each haem group exist an iron atom that is responsible for covalent bond (without change its valence) with O<sub>2</sub>. It can also create reversibly bonds with other ions, especially diatomic gaseous ligands, such as CO<sub>2</sub>, carbon monoxide (CO), nitric oxide (NO), nitroxyl (HNO), nitrite (NO<sub>2</sub>), hydrogen sulfide (H<sub>2</sub>S), but also water (H<sub>2</sub>O), cyanide, cyanate, thiocyanate, azide and fluoride. This protein can bind to a total of four O<sub>2</sub> molecules per haemoglobin, and the cyclic affinity states between them allows the O<sub>2</sub> binding and unbinding, where affinity is higher in the oxygenated state.<sup>60,61</sup>

To obtain information about the O<sub>2</sub> saturation levels and its balance in tissues, the measurement of haemoglobin states is performed at the level of microvasculature. However, alterations in the vascular compartments (capillary, arterial and venous) can influence the

variation of oxyhaemoglobin and deoxyhaemoglobin concentrations, since blood distribution compromises the tissue O<sub>2</sub> saturation.<sup>14,59</sup> Other examples of variables that can influence the measurement and interpretation of this chromophore states are: (i) stronger hypercapnia, with the baseline perfusion increased by up to 100%, reduce deoxyhaemoglobin response almost to disappear;<sup>59</sup> (ii) the excess of deoxyhaemoglobin is significantly reduced or even eliminated under normobaric or hyperbaric O<sub>2</sub> conditions, respectively, in situations of hyperoxia;<sup>59</sup> (iii) temperature variation influences the affinity balance between haemoglobin and O<sub>2</sub>, because the oxygenation of this molecule is an exothermic reaction, and, therefore, during hyperthermia the affinity decreases abruptly and during hypothermia the affinity increases, and deoxyhaemoglobin reduces;<sup>59,62</sup> (iv) the existence of nonheme ligands in haemoglobin, that are heterotropic effectors, influence the affinity of this protein to O<sub>2</sub>, because it changes the functional and structural modulation during the binding process in haem group, remaining the haemoglobin in the deoxygenated form;<sup>60,63</sup> (v) blood velocity is correlated with the variation in oxyhaemoglobin, deoxyhaemoglobin and haemoglobin total measurements.<sup>59</sup>

#### **2.1.2.2. Cytochrome c-oxidase**

This cytochrome c-oxidase is an enzyme of the terminal complex of the respiratory chain and uses more than 90% of the cell's oxygen consumption in a catalyse reaction to convert the oxygen molecule into water by transferring photons to it. Even if its concentration in vivo is only 10%, or less, of the existing haemoglobin, this enzyme can be measured with NIRS technology, providing important information about the cellular oxygen metabolism activity and mitochondrial functionality, oxygenation and oxidative metabolism.<sup>59,64–69</sup> Cytochrome c-oxidase is formed by four redox active metal centres, two haem (cytochrome a and a<sub>3</sub>) and two copper (Cu<sub>A</sub> and Cu<sub>B</sub>).<sup>70,71</sup> It has a characteristic absorption spectrum for visible and near-infrared light that are dependent of its redox state (absorption spectrum in NIR range of 680-980nm).<sup>59,67,68,71</sup> The Cu<sub>A</sub> is the best choice to reflect cytochrome c-oxidase and monitor this enzyme turnover at the near-infrared 830nm band.<sup>70,71</sup>

Cytochrome c-oxidase is, with haemoglobin, the chromophore of interest to be measured with NIRS, but it is not routinely assessed, and its interpretation and detection are difficult.<sup>59,65–67,70</sup> To overcome the difficulties of overlapping information and signal-to-noise ratio, a broadband NIRS system is used to accurately isolate the cytochrome c-oxidase attenuation signal from the spectroscopic signal contribution of haemoglobin. A multiple source-detector with longer separation than the ones usually used for haemoglobin measurements is also needed, since the signal of this enzyme is depth-dependence, and its NIRS values are not base in the signal provided by haemoglobin.<sup>66,70,71</sup> New algorithms are being developed and studied to simplify the analysis of redox cytochrome c-oxidase, and to improve the calculations of this enzyme, which are sometimes erroneous when only using the Modified Beer-Lambert law.<sup>59</sup>

## 2.2. Principles related to NIRS spectrometers

NIRS devices use multiwavelength algorithm, which is composed by algebraic expressions, to organize and separate all the overlapping information about the haemoglobin states and cytochrome c-oxidase captured by the photo detectors. To generate these algorithms a minimum of four near-infrared wavelengths are required.<sup>7,14</sup>

The photons emitted with near-infrared light, from the light source, will not be directed to the photodetector, nor in a straight path in substances like biological tissues, because light is constantly changing of path due to scattering effect. The optical pathlength is influenced by the mean and the distance of optodes. In the case of biological tissue, its characteristics will result in a pathlength with “banana or boomerang-shaped” curve beneath the sensor, forming an elliptical path from an optode to the other (figure 5).<sup>3,14,15,42,72</sup>

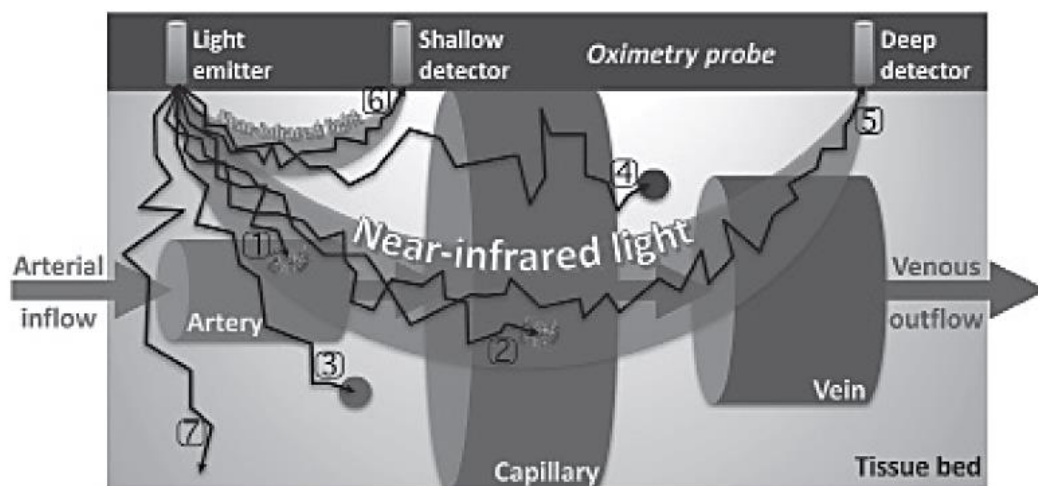


**Figure 5** - Technical details of tissue oximetry with near-infrared spectroscopy (NIRS) in reflectance mode: pathlength of near-infrared light, when emitted and received by the optodes of NIRS probe, in tissue bed (the size of the cross-section area of each different vessels depends of blood flow velocity, where capillary is the largest because is the slowest) and light travelling (line 1 and 2 - absorbed by haemoglobin, line 3 and 4 – absorbed by other existing chromophores, line 5 – received by deep detector, line 6 – received by shallow detector, line 7 – light lost).<sup>72</sup>

The photodetector is important to correlate optical pathlength with the inter-optode spacing. It uses the time that a photon takes to pass through the tissue and be detected by the sensor, and relates it to the distance that the same photon has travelled and the level of scattering it has suffered.<sup>14</sup>

The optical pathlength is directly related with the distance between the emitter and the receiver optode, but the spacing variability of light source and the detector also influence the

depth of photon penetration in the tissue sample, affecting light ray distribution and the amount of tissue monitored.<sup>42</sup> The depth that light beam can penetrate the tissue is approximately half of the distance between the emitter and the receiver optode in the NIRS probe, and the pathlength that photons travels is four to six and half times longer than the light source-detector distance, depending on the tissue irradiated (differential pathlength factor).<sup>14,49,73</sup> The probe can have different spacing distances between the light source and the photodetector, which vary the volume of tissue monitored under the sensor. The ideal distance, and the most widely used, is four centimetres (4 cm), but the devices can vary the inter-optodes distance between two and seven centimetres (2-7 cm), being the range of three to five centimetres (3-5 cm) the most frequently used in NIRS devices.<sup>48,59,73</sup> The distance of the source-detector optodes allows to measure and estimate the regional O<sub>2</sub> saturation of the tissue about one cubic centimetre (1 cm<sup>3</sup>) in volume, with a tissue penetration depth of two to three centimetres (2-3 cm).<sup>73</sup> The use of longer distances between the light source-detector optodes would help to reduce the influence of shallow tissues in the light received, which are not the focus for the tissue monitoring. However, a fast deterioration of the light signal would occur with the separation of the optodes.<sup>48,59</sup> Therefore, it's important to choose the correct NIRS sensor with the proper light source-detector distance, for achieving the best results when monitoring the targeted tissue.

The structures of the superficial tissues are not of interest to NIRS monitoring but can influence the measurements results. To separate the signal contribution received from the superficial (skin and subcutaneous tissue) and the deeper tissues (brain and muscle), it was developed a multi-distance approach where, in the same probe, it is used one or more photodetectors with different distances from the light source. Using more detectors allows the system to measure at different depths and, consequently, determine the type of tissue with depth.<sup>3,14,30,48</sup> According with the principle of spatial resolution, the detector closest to the light source will capture the light signal from more superficial tissues, while the distant optode receiver will measure deeper, but also superficial, tissues (figure 5).<sup>3</sup>

### **2.3. NIRS Spectrometers**

The basic components of NIRS monitoring devices are a sticker probe<sup>14</sup> with one or more light source (light-emitting diode - LED light, or laser diode)<sup>14,30,42,48,59</sup> and photodetectors,<sup>14,42,48,59</sup> photo detection hardware (photomultiplier and diverse amplifiers that convert light incident photons into an electrical signal),<sup>14</sup> computer (with software for algorithm processing and ability to translate the information of the emitted and recovered light into clinical information),<sup>14,42,48</sup> information display system,<sup>14</sup> and fiber optical bundles,<sup>14</sup> wireless system or multi-channel wearable<sup>74</sup> to transmit information between probe and computer.

There are three main methodologies of near-infrared light spectrometers defined by the light source and illumination method: continuous wave (CW), frequency domain (FD) and time domain (TD).<sup>15,48,50</sup> Continuous intensity NIRS (CW-NIRS) devices emit a continuous wave of constant intensity and it solely measures the intensity of the re-emerging light transmitted by the tissues.<sup>1,75,76</sup> The frequency domain NIRS (FD-NIRS) technique spectrometer is based in the frequency modulation, where the intensity of the light emitted from the source is modulated by a sinusoidal function in a particular frequency (usually radio frequency), and its range can vary from 50MHz to 1GHz. This enhanced technique measures the intensity of the attenuation light emitted by the tissues, the phase shift and the amplitude of modulation.<sup>34,50,75,76</sup> Timed domain NIRS (TD-NIRS) technology is characterized by measuring the time flight of photons, that travels through the tissue, and separate the information from superficial and deep tissues.<sup>77</sup> It uses ultra-short pulsed light sources, that are electromagnetic waves of light classically emitted with a time duration of picoseconds (equal to  $1 \times 10^{-12}$  seconds), but it can also be formed by using laser pulses of femtoseconds (equal to  $1 \times 10^{-15}$  seconds).<sup>34,77,78</sup> Exist two detection methods for TD-NIRS, using a streak camera or the technique of timed-correlated single photon counting (TCSPC).<sup>50,77</sup> The inclusion of a streak camera was the first development of TD-NIRS, and it detects the intensity of the emitted light in different locations of the measured tissue. The development of TCSPC method allowed to detect the photons received from the emitting light, and distinguish and order them according with their time of arrival. This is characterized as the "impulse response" of the tissues, and helps to determine their optical properties.<sup>50</sup>

The CW system is the most used due to its low cost, easy transportation, less complexity and for being an easy and simple technology to use.<sup>1,34,74,76</sup> The FD and TD techniques are more accurate, and give the absolute characterization of tissues' optical properties, and absolute values of oxygenated and deoxygenated haemoglobin concentrations.<sup>74</sup> They include absorption and scattering coefficients, which allows these measurements, while the CW system cannot determine these coefficients and, consequently, the absolute values.<sup>1,34,75,77</sup> The FD and TD-NIRS systems are limited in daily practice, due to their complexity, high costs and because they are still not suitable for clinical environment, being mainly used in research projects.<sup>15,34,75</sup>

There are several NIRS spectrometers available in the market, with different characteristics, equipment, measurement methods (spatially resolved spectroscopy)<sup>56-58,79-81</sup>, methodologies (diffuse correlation spectroscopy)<sup>82-84</sup> and techniques (functional near-infrared spectroscopy).<sup>1,74,84-89</sup> It is important to choose the right NIRS device, depending on the information that is needed to collect, in order to guarantee a high signal-to-noise ratio and avoid overlapping information. Also, selecting the appropriate wavelength, light source, detectors and geometrical arrangements help to overcome the existing limitations and to reduce the influencing factors.<sup>1,34,46</sup>

## 2.4. Limitations in near-infrared spectroscopy measurements

- Influence of other chromophores in light attenuation

Before the near-infrared light emitted reach the tissue of interest, it passes through heterogenous layers of tissue, with variable scattering and absorption effect due to the different tissue-derived chromophores, the volume of blood and the type of tissue present.<sup>48,90</sup> Besides the haemoglobin and cytochrome c-oxidase, which are the chromophores of interest, the other existing molecules capable of absorb near-infrared light may also contribute to NIRS readings, and have some competitive effect in absorbing the emitted light. That chromophores are melanin,<sup>7,30,48,59,90</sup> bilirubin,<sup>48,90,91</sup> collagen, myoglobin,<sup>14,30,48</sup> water,<sup>1,48</sup> and lipids<sup>1,48</sup> (figure 6). Some of these molecules may have higher absorption coefficients in the near-infrared light range than the chromophores of interest, but their contribution is reduced because they exist in low concentrations compared to haemoglobin. These chromophores will be responsible for absorb a minimum value of the near-infrared light emitted and will contribute less than haemoglobin for the light signal captured. Haemoglobin is considered the main absorber responsible for the results obtained by NIRS.<sup>1,7,30</sup>

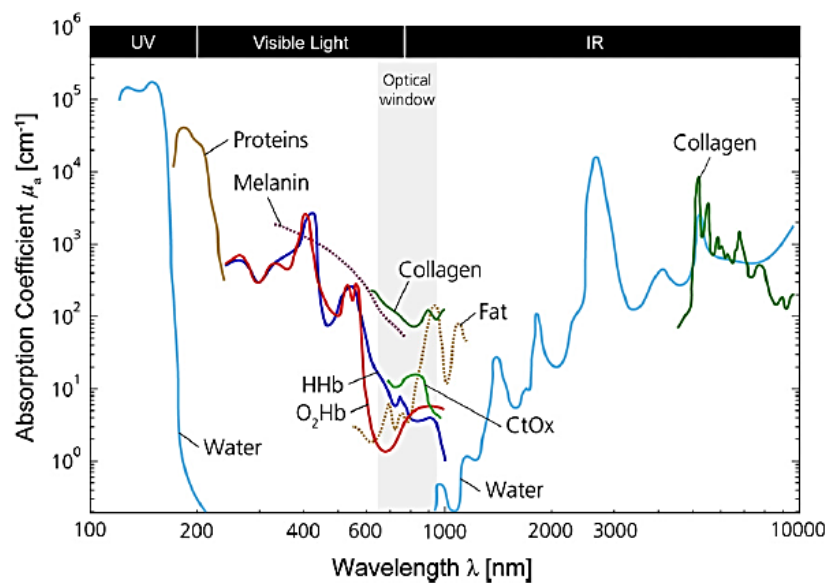


**Figure 6** – Absorption spectra, in logarithm base, for the different chromophores present in biologic tissue that can influence Near-infrared spectroscopy measurements, with the representation of the “optical window” to use in this monitoring.(O<sub>2</sub>Hb – oxyhaemoglobin, HHb - deoxyhaemoglobin, CtOx - cytochrome c-oxidase).<sup>1</sup>



- Undefined optical pathlength

The algorithms used in NIRS calculations assume a fixed distance value for light's optical pathlength, but there are many factors that influence the path that each photon takes to travel through the tissue sample. The type of tissue, the interindividual variation in tissues components, the wavelength used, the scattering coefficient of the mean, the optode geometry, probe positioning and the changes and variations of blood volume, can change photons trajectory and create a distribution of paths instead of a unique direction.<sup>3,48</sup> It is assumed that the pathlength travelled by the emitted light is in banana-shaped between source-detector optodes of the probe but, in reality, the path that the light follows is much longer than the distance between optodes. Since the measurement of the true optical pathlength can vary in 10 to 15% of the true distance, it was created a parameter in order to adjust the calculations that include the extra distance travelled beyond the distance between the optodes.<sup>3,92</sup> The differential pathlength factor is the parameter that was included to allow a more accurate estimation/measurement of the optical pathlength distance. However, it is a wavelength-dependent factor that decreases with increasing wavelength, and it is mainly influenced by scattering effect and depends on optodes geometry. It can be measured by using FD-NIRS or by measuring the mean time of flight of a picosecond pulse of near-infrared light when it passes through biological tissue (TD-NIRS), but, if this parameter is not accurately measured, cross talks of the information obtained can occur.<sup>48,92</sup>

- Near-infrared light lost that is unknown due to scattering effect

Scattering effect is difficult to quantify in an absolute value, which leads to an unknown light loss (scattering loss factor) when near-infrared light passes through biological tissues. The existing models used in NIRS technology only allow to predict and approximate to the value of the scattering loss factor.<sup>48</sup>

- Extracranial tissue contamination, including the thickness of skull and cerebral fluid in brain monitoring<sup>48,51,90,91</sup>

It is difficult to separate the NIRS signal from the brain from the extracerebral tissue, which is formed by the scalp, temporal muscles, skull, frontal sinus, cerebrospinal fluid and dura.<sup>91</sup> The distance between skin and cerebral tissue difficult the brain measurements by NIRS devices because of their deep range. It is important to control the patient's positioning since changes in the patient's position may influence the thickness of cerebrospinal fluid. Also, the NIRS sensor must be placed where the thickness and number of tissue layers are reduced in order to decrease the distance between the sensor and the cerebral tissue.<sup>90,91</sup> The variation of the distance between the optodes of NIRS sensor can help to reach a greater depth range and, consequently, reduce the effect of extracranial tissue. However, with the increase of source-detector distance

the signal intensity will be smaller and can difficult the detection of the light by the photodetectors.<sup>90</sup>

- Other limitations to take into consideration

Placing the probe over a hematoma, oedema (or areas that easily can form oedema), thick layers of adipose tissue, bone or over pigmented areas.<sup>7,30,51</sup>

Variation of arterial/venous ratio and situations of hypoperfusion or hyperperfusion may influence the measurement.<sup>3,90,91</sup>

Depth measurement capacity influenced by the source-detectors distance, the number of detectors and the wavelength used.<sup>59,90</sup>

Fluctuations in body temperature and excessive movement induce errors in measurements.<sup>7</sup>

External light source as an artefactual factor.<sup>3</sup>

In veterinary patients there is a lack of standardized reference values between NIRS devices and measuring sites. And, in some species such as cats, there are no published reference NIRS values for monitoring microcirculation.<sup>7</sup>

## **2.5. NIRS significant value to standard anaesthetic monitoring**

Briefly, NIRS technology is used to measure the absorption of near-infrared light by the tissues and blood, to provide information about the balance of O<sub>2</sub> supply and consumption, by assessing microvasculature, and the metabolism activity (by monitoring O<sub>2</sub> utilization) through the redox state of cytochrome c-oxidase present in intracellular space.<sup>31</sup> The aims of this technology are to quantify the concentration of the chromophores responsible for O<sub>2</sub> saturation and monitoring physiological demands and deficits to maintain homeostasis, by clinical approaching pathological changes as early as possible.<sup>50,72</sup>

NIRS measurements are continuous, real time and do not depend on cardiac cycle or even to capture a quality signal from pulsatile flow, like pulse oximeter.<sup>3,14,73</sup> This last one uses systolic and diastolic cycles and absorption values to measure arterial O<sub>2</sub> saturation and to create the plethysmograph pulse waveform.<sup>3,14</sup> NIRS can assess O<sub>2</sub> saturation in different vascular components (capillary, veins, venules, arteries and arterioles) and the nonpulsatile optical components, monitor a specific organ or tissue of interest (muscle or brain for example) and measure other parameters besides haemoglobin saturation (cytochrome c-oxidase<sup>66</sup> and tissue

O<sub>2</sub> index - TOI%,<sup>79</sup> for example).<sup>3,14,73</sup> NIRS provides a noninvasive monitoring tool that allows assess the regional and global tissue perfusion and circulatory function, that makes possible to evaluate and monitor the imbalances between tissues' O<sub>2</sub> supply and metabolic demands.<sup>3,73</sup> Thus, NIRS allows to early identify ischemia events in organs and tissues that can be pass unnoticed otherwise, until clinical signs of organ dysfunction become evident.<sup>3,14</sup> Due to the estimation of systemic venous saturation and the correlation of this parameter with circulatory status, NIRS is a valuable tool for early detection of deficits in perfusion and prevent organ morbidity, mortality and/or neurologic outcomes.<sup>3,73</sup>

## 2.6. Near-infrared spectroscopy monitoring

NIRS information cannot be used alone and is necessary to include it in a multimodal monitoring strategy, because cerebral and somatic NIRS information can alert about perfusion and oxygenation alterations but cannot indicate the mechanism or aetiology that induced the eventual desaturation.<sup>91</sup> When NIRS values decrease, it is important to rule out any technical or mechanical problem, such as inappropriate and incorrect positioning of NIRS sensor, by checking the equipment, head positioning, and evaluating if there is any problems associated with application or malpositioning of surgical instruments (arterial or venous cannula used in extracorporeal circulation procedures, for example).<sup>3</sup>

The use of NIRS technique for cerebral monitoring<sup>15,30,41,90,93-95</sup> was the most studied and developed area, being followed by muscle tissue oxygen saturation monitoring. NIRS also started to be used and applied to transcutaneously measure the oxygenation of the kidney,<sup>15,96,97</sup> intestine,<sup>15,98-101</sup> liver,<sup>99,102</sup> splanchnic tissue,<sup>98-101,103</sup> and testicles<sup>104</sup>, due to the superficial location of these organs. Each tissue and organ have its own metabolic rate, basal oxygen extraction and demands (figure 7).<sup>3,105</sup> In situations where homeostasis and organs metabolic needs are compromised, the blood flow and oxygen extraction increase to compensate this imbalance and the non-vital organs, as kidneys, intestine and liver, may enter in a state of occult ischaemia.<sup>3,105</sup> Although NIRS monitoring in these tissues are not validated nor used as standard clinical applications, studies have been

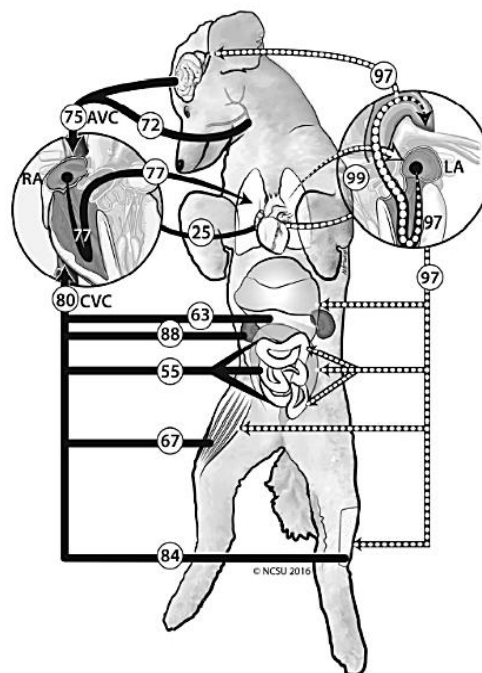


**Figure 7-** Representative values of oxygen saturation in different tissues in a dog model, where the arterial values are identified through dotted lines and the venous values by solid black line.<sup>105</sup>

demonstrating positive results when using NIRS technology to monitor organ tissues in patients under 10 kilograms, neonates and infants.<sup>3,15,30,99</sup>

### **2.6.1. NIRS in skeletal muscle monitoring**

When NIRS technique was developed, due to its monitoring features and to the information that the clinicians can obtain regarding the oxygenation of peripheral tissues, the muscle NIRS evaluation started to be implemented and studied in order to be used as an early indicator of hypoperfusion and tissue hypoxia.<sup>31,34,106,107</sup>

The NIRS values obtained during skeletal muscle monitoring are a reflection of the muscle microcirculation, where capillaries are the main source of the total blood volume in muscle tissue (>90%), and a reflection of the intracellular myoglobin concentrations.<sup>108</sup> Human<sup>109–112</sup> and animal<sup>112–114</sup> models studies showed that NIRS information generally follows the alterations occurred in venous blood O<sub>2</sub> saturation, but also alerted for some discrepancies that may occur due to the intracellular myoglobin and blood volumes changes, which alters the O<sub>2</sub> gradient between arteries and venules.<sup>31,34</sup> It is estimated that 70% of the total amount of blood in the organism is in the venous compartment (with, approximately, 75% of the total venous blood located in the small veins (30%) and venules (45%)). The remaining 30% of the whole blood is located in the arterial compartment, with a venous:arterial blood volume ratio of 2.33.<sup>109,115</sup>

The skeletal muscle can obtain energy (ATP production) for its functions through aerobic mechanisms, such as oxidative phosphorylation, and through anaerobic processes when the O<sub>2</sub> is not sufficient to supply the metabolic needs. Since the main source of energy is the aerobic route through oxidative mechanism, and the skeletal muscle is a peripheral tissue that can be easily assessed for monitoring, NIRS can be used for monitoring the local muscle O<sub>2</sub> balance (supply and consumption) and the blood flow.<sup>34</sup> Jobsis was, in 1977, the pioneer in using NIRS technology for medical application,<sup>37</sup> and he extended his research to skeletal muscle NIRS monitoring,<sup>116,117</sup> by studying the cytochrome c-oxidase and the skeletal muscle O<sub>2</sub> concentrations response to NIRS technology.<sup>34,118</sup> In the end of 1980, NIRS technique started to be used to measure muscle oxidative metabolism in different scenarios (resting and during muscle activity).<sup>119</sup> Wilson, *et al.*, 1989<sup>112</sup> showed that NIRS could detect changes on skeletal muscle oxygenation, and suggested that NIRS technology had the potential for being used as a valuable method for monitoring muscle O<sub>2</sub> delivery, assessing blood flow impairments, and assessing the

effects of therapeutic interventions. Since the 1990's, the NIRS oximeters were capable of measuring O<sub>2</sub> supply-demand balance in superficial muscles (figure 8).<sup>108</sup>

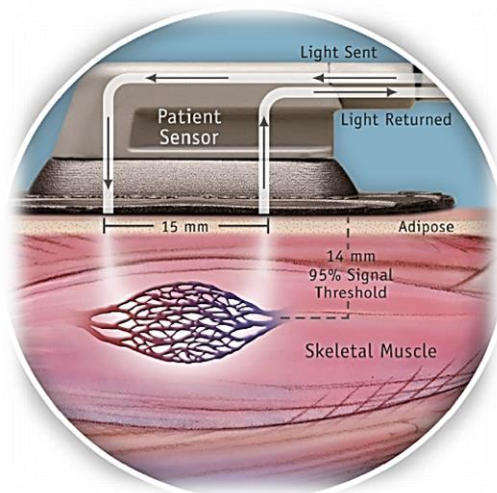


**Figure 8** - Representation of skeletal muscle oxygen saturation measurement with near-infrared spectrophotometry, placed above the tissue bed.<sup>121</sup>

By using NIRS technology for the measurement of skeletal muscle tissue O<sub>2</sub> saturation, both in human and veterinary medicine,<sup>7</sup> it became possible to detect occult shock and predict its severity,<sup>114,120</sup> to provide more accurate prognostic information, improve patients' triage in emergency settings, improve patients' outcomes during resuscitation,<sup>114,121</sup> detect myopathies (important in equine clinic),<sup>122</sup> and to monitor peripheral perfusion and tissue hypoxia when other monitoring techniques are not indicated, such as central/mixed venous oximeters.<sup>7</sup>

The variability in muscle NIRS readings with gender, age, size/weight and body mass index have been reported.<sup>31</sup> Studies performed in dogs showed that age<sup>41</sup> and body mass index<sup>123,124</sup> (but not gender<sup>41,123,124</sup> or size/weight<sup>41,124</sup>) can influence the muscle NIRS readings. Although there were no differences between male and female dogs' NIRS measurements in the various muscular sites tested,<sup>41,123,124</sup> the possibility that neutered animals might have influenced the results was raised.<sup>123</sup>

Skeletal muscle NIRS measurements can be influenced by increasing body mass index, which leads to a decreasing in the tissue O<sub>2</sub> saturation and, consequently, to a decrease in NIRS values.<sup>123,124</sup> A study that evaluated the O<sub>2</sub> saturation measurements with NIRS in the sartorius muscle in seventy-eight healthy adult dogs, reported significant differences in the NIRS values between dogs with a body mass index of 5 to 5.5, and dogs mildly to severely overweight with body mass index of 6-6.5, and above 7.<sup>123</sup> Relatively to age parameter, a study performed in dogs in a population of forty-eight Chihuahua reported a small positive linear relation between age and femoral muscle NIRS measurements.<sup>41</sup> The clinical importance of the linear correlation reported in this study<sup>41</sup> is questionable.

The positioning of patient, standing or lateral recumbency, and the placement of probe on the left or right side, have no effect on the muscle NIRS measurements.<sup>124</sup>

#### 2.6.1.1. Muscle sites for NIRS measurement in animals

The skeletal muscle NIRS readings will not mainly represent the haemoglobin O<sub>2</sub> saturation and O<sub>2</sub> balance, due the existence of myoglobin that shares similar optical properties with haemoglobin, which decrease the accuracy of the results and influence the light attenuation.<sup>30,31</sup> Melanin and elevated blood volume are also responsible for reducing the penetration depth of near-infrared light and the reflected light intensity, which limit the range distance of NIRS measurements.<sup>34</sup> For these reasons, it is important to perform the measurements in a muscle location where the influence of these limiting factor is almost null. However, there is a limited number of studies about NIRS monitoring in veterinary medicine, NIRS range of values and measurement sites, being the dog the most studied animal.<sup>124</sup>

The most recommended site to measure muscle O<sub>2</sub> saturation with NIRS technique in dogs is the sartorius muscle.<sup>7,123,124</sup> Most of the articles that use and defend this location are based on the results of the study performed by Hall, *et al.*<sup>123</sup> in 2008, with a population of seventy-eight healthy adult dogs, weighting above nine kilograms. The sartorius muscle is located on the cranial medial aspect of the thigh and can easily be assessed (figure 9). The NIRS sensor is easy to be applied on the skin over the sartorius muscle, that has usually no pigmentation, has little hair and a small layer of subcutaneous fat tissue, when comparing to other muscles (vertebral lumbar epaxial muscle, a region where subcutaneously adipose tissue is usually present).<sup>123,124</sup> The NIRS measurements over the sartorius muscle presented the most consistent readings, with a success rate of 100% in obtaining tissue O<sub>2</sub> saturation measurements, when compared to 70% and 67% of consistent readings from the other muscular sites tested: forearm digital extensors and biceps femoris muscles, respectively.<sup>123</sup>



**Figure 9** - NIRS (near-infrared spectroscopy) sensors placed over the sartorius muscles of a dog, using two different NIRS devices: INVOS™ (right leg) and Inspectra™ (left leg).<sup>124</sup>

The sartorius muscle in dogs is usually supplied by branches of the superficial circumflex iliac and lateral circumflex femoral arteries (sartorius proximal portion), muscular branches from the femoral artery (sartorius middle portion), and muscular branches from the descending genicular artery (sartorius distal portion) (figure 10).<sup>125</sup>

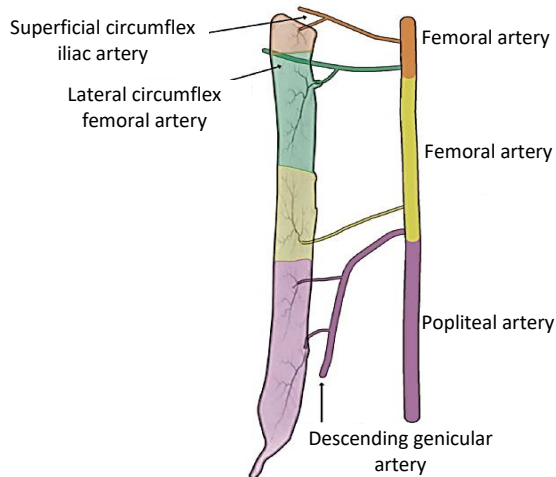


**Figure 10** - Scheme of sartorius muscle with its arterial supply in canine topographic anatomy. Adapted from<sup>125</sup>

Another possible measurement site reported for muscle NIRS monitoring is the gracilis muscle. Some animal studies focused in NIRS measurements over this muscle,<sup>41,112,117,126,127</sup> located subcutaneously on the caudal aspect of the medial thigh.<sup>125,128</sup> However, only two studies addressed the NIRS measurements in the gracilis muscle,<sup>41,112</sup> while the other studies were focused in evaluating NIRS variations.<sup>117,126,127</sup> Wilson, *et al.*, 1989,<sup>112</sup> reported NIRS value of  $73.3 \pm 4.3\%$  for venous haemoglobin O<sub>2</sub> saturation and  $93.4 \pm 1.1\%$  for arterial haemoglobin O<sub>2</sub> saturation from the gracilis muscle in five dogs, at rest. Hiwatashi, *et al.*, 2017,<sup>41</sup> reported mean NIRS values of  $67\% \pm 6\%$  for regional oxygen saturation on gracilis muscle in a population of forty-eight Chihuahuas, using the Toccare finger mounted NIRS device.

When comparing the anatomical characteristics of the gracilis and sartorius muscles, the first one is only vascularized by the proximal caudal femoral artery and, in cats, also by collateral branches of saphenous artery. When compared to sartorius architectural muscle index (average muscle fiber length divided by the average muscle length), the gracilis muscle has a muscular index value lower in dogs and higher in cats. Gracilis is thicker than sartorius muscle, and it has greater muscle mass and physiological cross section area.<sup>128-130</sup> These anatomic differences between gracilis and sartorius muscles may be the reason behind the significantly difference performance of NIRS monitoring in the sartorius and gracilis muscles.

### 2.6.1.2. Normative NIRS values and variability factors

For an accurate identification of hypoperfusion and tissue hypoxia, it is important to predefine a cut-off value for tissue O<sub>2</sub> saturation (StO<sub>2</sub>), which is the minimum value of tissue O<sub>2</sub> saturation that assures an adequate organ perfusion. The cut-off value is an intervention indicator used as a significant predictor of outcomes for multiple organ dysfunction syndrome and patient death in humans. The values are determined through logistic regression analyses, and the range reference recommended for cut-off StO<sub>2</sub> values in humans is of 70% to 75%.<sup>123,131</sup>

Hall, *et al.*<sup>123</sup> established in 2008 a reference normal NIRS range for dogs (71% to 99%) as baseline for normal tissue O<sub>2</sub> saturation level measured in the sartorius muscle.<sup>123</sup> However, a study performed in healthy dogs using different NIRS devices (Inspectra™ and INVOS™) reported very distinct cut-off values. When using the Inspectra™ device, the recommended NIRS cut-off value was 78%, below which the clinician should consider an early identification of perfusion compromising and early organ dysfunction.<sup>124</sup> On the other hand, when using the INVOS™ device, the NIRS mean values obtained for healthy dogs were all under the cut-off value recommended for the Inspectra™ device.<sup>124</sup> Thus, it is not possible to use an universal cut-off value for all NIRS devices in dogs, and it is crucial to establish a reference range for StO<sub>2</sub> readings and a cut-off value for each monitor, in order to avoid misinterpretations of the NIRS values. It has been suggested that the cut-off value should be the NIRS value two standard deviation below the mean values of the tissue O<sub>2</sub> saturation value obtained by each different NIRS device from healthy subjects.<sup>124</sup>

Several other factors, besides species, age, body mass index, fat, evaluated site, biological needs and individual variability, have been reported to influence NIRS values.<sup>15,31,34,41,105,123</sup> Sullivan, *et al.*, 2011<sup>132</sup> suggested the altitude as an influencing factor for the lower NIRS values obtained, regardless of the different anatomical locations used for the NIRS measurements (the abdominal wall near the linea alba, and the inguinal area). Another influencing factor is the presence of myoglobin in muscle tissues, with studies suggesting a 90% contribution to the NIR signal by this molecule.<sup>34</sup> Also, the summation of information from arteries, venules and capillaries O<sub>2</sub> saturation, used by the NIR signal, can vary according to the blood volume from the arterial and venous systems, which can erroneously reflect changes in venous blood O<sub>2</sub> saturation.<sup>34,118</sup>

### 2.6.2. Total haemoglobin index

The total haemoglobin index (THI) represents a metric signal strength of the haemoglobin, providing information regarding vasodilatation, and is measured by NIRS devices while StO<sub>2</sub> is measured.<sup>7,123,133,134</sup> The THI values (unitless values between 1 and 99) does not indicate the blood haemoglobin concentration, on the contrary. It represents the total amount of haemoglobin in a determined volume of tissue that is monitored by the NIRS method.<sup>7,123</sup> The THI is obtained



through an algorithmic function of NIRS device software, and represent an estimative of oxyhaemoglobin and deoxyhaemoglobin quantity per unit area in the microcirculation blood flow on the monitored tissue.<sup>41,133</sup>

Studies performed in dogs showed that monitoring StO<sub>2</sub> associated with THI may yield similar results to those published in human studies.<sup>41,123</sup> Hiwatashi, *et al.*, 2017,<sup>41</sup> report that cerebral THI values are higher than those obtained for femoral skeletal muscles. These same authors was also reported the existence of a positive correlation between body weight and muscle THI, a negative slope between body weight and cerebral THI, and no influence of age in the THI values.<sup>41</sup> Further investigations to validate the use of this parameter and its meaning in animals and in different organs are considered necessary.<sup>41,123</sup>

## **2.7. NIRS monitoring in veterinary practice in cats**

The studies published about NIRS monitoring in animals are sparse and refer to different species, such as mice,<sup>42,86,104,135</sup> rabbits,<sup>42,120</sup> cats,<sup>37,117,127,136–138</sup> dogs,<sup>37,41,42,94,112,113,123,124,132,139,140</sup> pigs,<sup>95,100,102,114,141</sup> horses,<sup>93,122</sup> lactating cows,<sup>142</sup> primates,<sup>143–147</sup> sheep,<sup>79,148–151</sup> goats,<sup>152</sup> marine mammals<sup>153</sup> and birds.<sup>154</sup>

The studies published addressing NIRS monitoring in cats are few, and the first study was published by Jobsis 1977,<sup>37</sup> where the transillumination of a cats' cranium with infrared light was proposed to monitor O<sub>2</sub> cerebral saturation. Mook, *et al.*, 1984<sup>138</sup> used near-infrared spectrophotometry and oxygen electrode techniques to compare its performance in assessing the effect of progressive hypoxia in cats in brain oxygenation. Piantadosi and Jobsis-Vander Vliet, 1985,<sup>117</sup> performed the first evaluation with near-infrared technique on intact biceps femoris and gracilis muscles in cats during controlled protocols of hypoxia and haemorrhagic hypotension. These authors studied the variation of cytochrome a, a<sub>3</sub> oxidation-reduction responses, myoglobin saturation and oxygenation changes during each protocol, and reported that the NIR values obtained from metabolic signals are feasible for evaluating oxygen saturation in resting skeletal muscle.<sup>117</sup> Another study, performed by Cairns, *et al.*, 1986,<sup>137</sup> reported the usefulness of using NIRS to assess brain metabolism and oxygenation in anesthetized female cats subjected to a protocol of increasing intracranial pressure. Accordingly to the collected NIRS data, these authors suggested an innovative therapeutic approach for head injuries, consisting in delivering 50% of O<sub>2</sub> associated with 5% of CO<sub>2</sub> during ventilation to improve brain oxygenation values.<sup>137</sup> Proctor *et al.*, 1988,<sup>136</sup> used the NIRS technique to detect metabolic events related with head injuries in cats to evaluate brain autoregulation mechanism in the postinjury period. The authors reported an increase of oxygenated blood flow associated to lethal closed head injury, and a loss of brain autoregulation and a deterioration of mitochondrial function in the postinjury period.<sup>136</sup> Hampson and Piantadosi 1990,<sup>127</sup> addressed the changes of O<sub>2</sub> availability in brain and skeletal

muscle (hindlimb, biceps and gracilis muscle) in anesthetized cats during hypercapnia and hypocapnia events, which induce respiratory acid-base imbalance in these cats. The authors of this study<sup>127</sup> concluded that NIRS was capable to rapidly detect and assess changes in O<sub>2</sub> levels measured continuously in multiple tissues. Also, hypercapnia induced progressive changes in both cerebral and muscle tissues NIRS readings, but with different NIRS response between cerebral and muscle tissue. During hypocapnia, it were observed cerebral NIRS values changes but there were no observed NIRS changes in the muscle tissue.<sup>127</sup>

To our knowledge, the latest study using NIRS monitoring in cats was published over 30 years ago, and there are no published studies addressing the sartorius muscle NIRS monitoring in healthy cats during routine surgical procedures. And during these 30 years, NIRS technology has evolved immensely towards a better performance during clinical practice.

### **III. Objectives for the study**

The objective of this study is to determine the NIRS range values in the caudal portion of the sartorius muscle in domestic female cats, during ovariohysterectomy. It will also be studied if NIRS is able to detect noxious stimulation, and to determine if NIRS values correlate to the physiological variables recorded during the surgical procedures in the same group of cats.

## **IV. Materials and Method**

### **Patients**

This study was performed in the facilities of the Centro Hospitalar Veterinário, Porto, Portugal, during routine elective ovariohysterectomy in cats who were patients from the hospital or referred from other veterinary clinics. The inclusion criteria were healthy female cats, of any age. Clinical evaluations (physical exam, blood analyses and clinical history) were assessed at the hospital before surgery or at the veterinary clinics prior to referral for surgery at the Centro Hospitalar Veterinário.

### **Anaesthetic protocol**

Cats were premedicated with intramuscular administration of dexmedetomidine, 10 µg/kg (DEXDOMITOR®, Orion pharma, Espoo, Finland), and ketamine, 2 mg/kg (Nimatek, Dechra, Northwich, United Kingdom), prepared in the same syringe. An intravenous catheter was introduced in cephalic vein and connected to a lactated Ringer's lactate solution (BRAUN VET, B BRAUN, Melsungen, Germany) fluid delivery line, at a delivery rate accordingly to the formula  $(30 \times \text{weight} + 70) / 24$  ml/hr.

Oxygen 100% was delivered via facial mask during surgical preparatory procedures. After trichotomy, intramuscular methadone 0.2 mg/kg (Semfortan®, Dechra, Northwich, United Kingdom) was administered. Induction of anaesthesia was performed with propofol 1% (PropoVet™, Zoetis, Parsippany, New Jersey U.S.) dose-effect. All patients were intubated and mechanical ventilated using Mindray WATO EX-20 Vet (Mindray Medical International Co., Ltd., Shenzhen, China) (figure 11). Ventilatory parameters were adjusted accordingly to each patient's needs, towards having peripheral O<sub>2</sub> saturation above 98% (SPO<sub>2</sub>>98%) and end-tidal carbon dioxide (EtCO<sub>2</sub>) between 35 and 45 mmHg values. Hypnosis was maintained with sevoflurane (SevoFlo, Zoetis Belgium SA, Louvain-la-Neuve, Belgium), with an initial vaporized concentration of 1.5%, and then adjusted to patients' needs. Fentanyl (Fentadon®, Dechra, Northwich, United Kingdom) was prepared for intraoperative rescue analgesic medication, if necessary.

### **Monitoring and data collection**

The study period was defined from five minutes after intubation (T0) until ending sevoflurane administration.

An O3™ Regional Oximetry® device (Masimo Corporation, Irvine, CA, USA) (figure 11) with an adult sensor was used for NIRS data collection. This device is able to measure the NIRS absolute value (with an accuracy of ±4% for adult sensor, and ±5% for paediatric sensor) and the

trend value of regional O<sub>2</sub> saturation (with an accuracy of  $\pm 3\%$ , when EtCO<sub>2</sub> values are not controlled, and with an accuracy of  $\pm 2.1\%$  with controlled EtCO<sub>2</sub> values).<sup>155</sup> The NIRS sensor was attached, after trichotomy of the monitoring area, to the skin over the caudal portion of the sartorius muscle of the cats' left leg.

The haemodynamic and ventilatory data was recorded using the Mindray BeneView T8 monitor (Mindray Medical International Co., Ltd., Shenzhen, China) (figure 11).



**Figure 11** - O3™ Regional Oximetry® device (Masimo Corporation, Irvine, CA, USA), Mindray BeneView T8 monitor and mechanical ventilator Mindray WATO EX-20 Vet (Mindray Medical International Co., Ltd., Shenzhen, China) used for this study at the Centro Hospitalar Veterinário. (Picture by Patrícia Moio)

The NIRS value (%), SpO<sub>2</sub> (%), heart rate (bpm), EtCO<sub>2</sub> (mmHg), sevoflurane minimum alveolar concentration values, temperature (°C), systolic blood pressure (mmHg), diastolic blood pressure (mmHg) and mean blood pressure (mmHg) were recorded every minute. During the ovariohysterectomy procedure, these variables were also recorded during several surgical moments prone to noxious stimulation: surgical towel clamp; skin incision; linea alba incision; left suspensory ligament rupture; left ovary pedicle ligature; right suspensory ligament rupture; right ovary pedicle ligature; uterine body traction; uterine body ligature; uterine body transection; closure of the linea alba; end closing linea alba; skin closure; end of skin closure.

### **Statistical analyses**

Pearson's correlation analysis was used to compare NIRS regional oxygen saturation (rSO<sub>2</sub>) values with the physiologic variable recorded. NIRS (rSO<sub>2</sub>) values were also compared at each surgical moment using Kruskal-Wallis analysis of variance. Statistical significance was defined when p-value < 0.05. Data are mean  $\pm$  SD. Statistical analysis was performed using SPSS version 25 software.

## V. Results

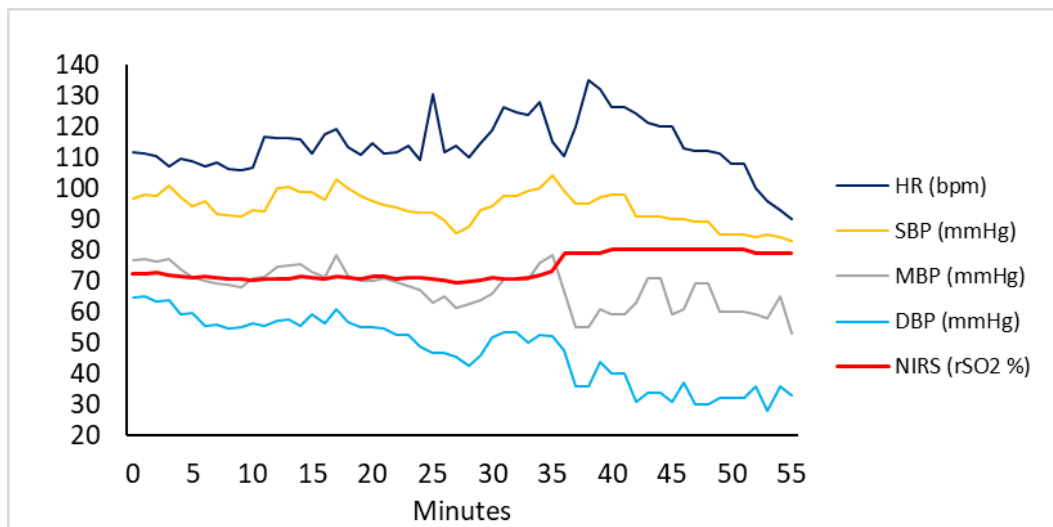
From the twelve cats enrolled in the study, six were excluded from analysis due to problems in accurately recording the arterial blood pressure values during the study period.

Six healthy domestic female cats, age  $6.00 \pm 1.55$  months, weight  $2.77 \pm 0.52$  kg, were analysed. The duration of the study period (from T0 to ending sevoflurane administration) was  $36.50 \pm 11.59$  minutes.

During the study period, the  $SPO_2$  and  $EtCO_2$  values were, respectively,  $98.17 \pm 0.42\%$  and  $42.57 \pm 0.57$  mmHg. Sevoflurane minimum alveolar concentration (MAC) values ranged from 0.57 MAC to 0.71 MAC. Heart rate (HR) was  $112.42 \pm 7.61$  bpm, systolic blood pressure (SBP) was  $95.55 \pm 3.04$  mmHg, mean blood pressure (MBP) was  $70.93 \pm 2.34$  mmHg and diastolic blood pressure (DBP) was  $55.14 \pm 3.17$  mmHg. Body temperature was  $37.03 \pm 0.12$  °C.

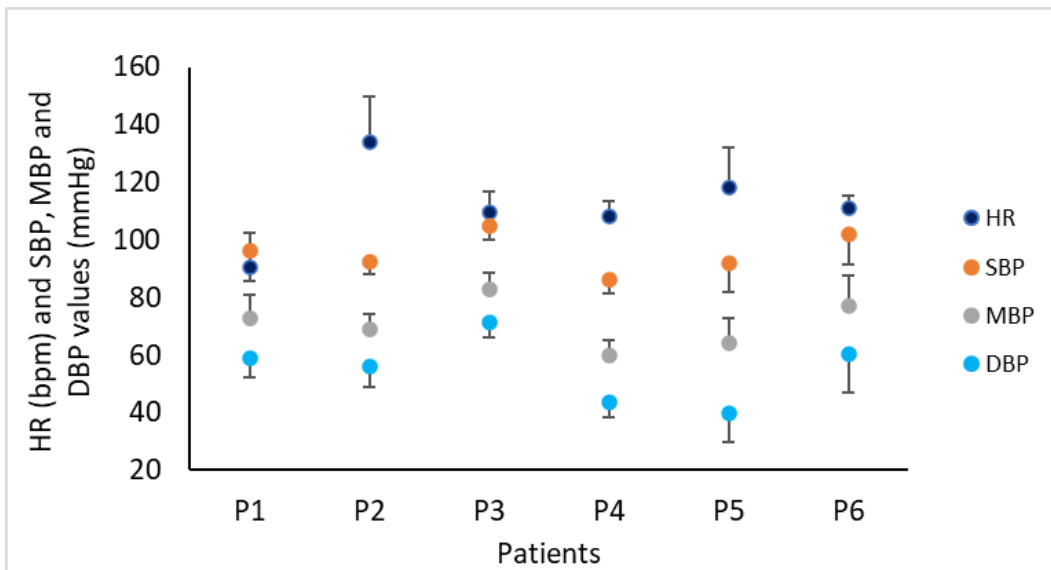
The NIRS ( $rSO_2$ ) values during the surgical procedure were  $71.84 \pm 4.85$  % (65% to 83%).

Graphic 2 shows the mean data of all patients during the study period. It is important to take into consideration the different duration of the anaesthetic periods between patients, as it is evident in the graphic 4.



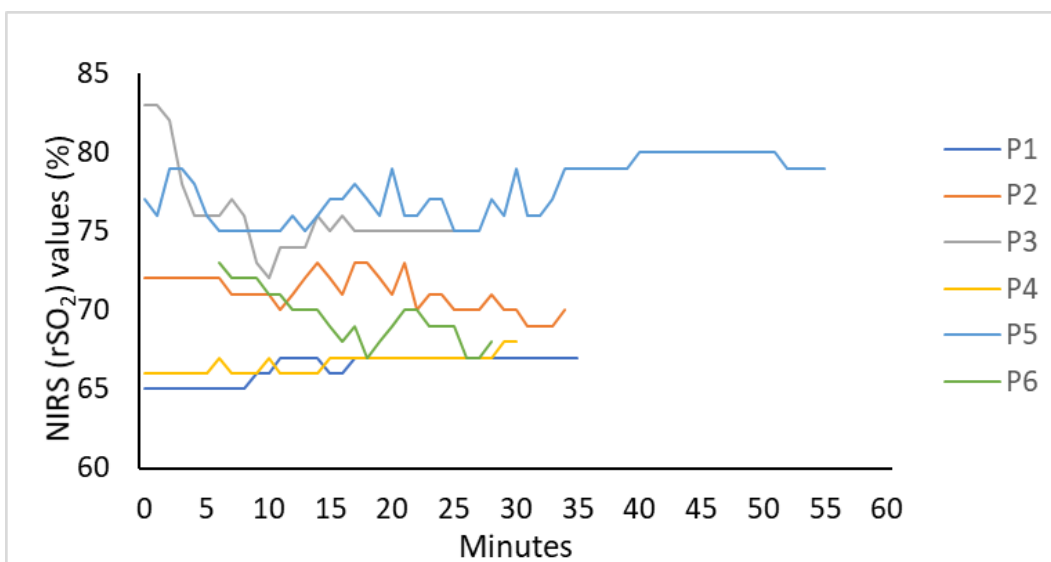
**Graphic 2** - Mean values of HR, SBP, MBP, DBP and NIRS from all patients from T0 until the end of sevoflurane administration. (HR- Heart rate; SBP- Systolic blood pressure; MBP- Mean blood pressure; DBP- Diastolic blood pressure; NIRS- Near infrared spectroscopy;  $rSO_2$ - Regional oxygen saturation).

As it can be observed in graphic 3, the standard deviation of the haemodynamic variables per patient during the anaesthetic period, can be considered within normal intervals.



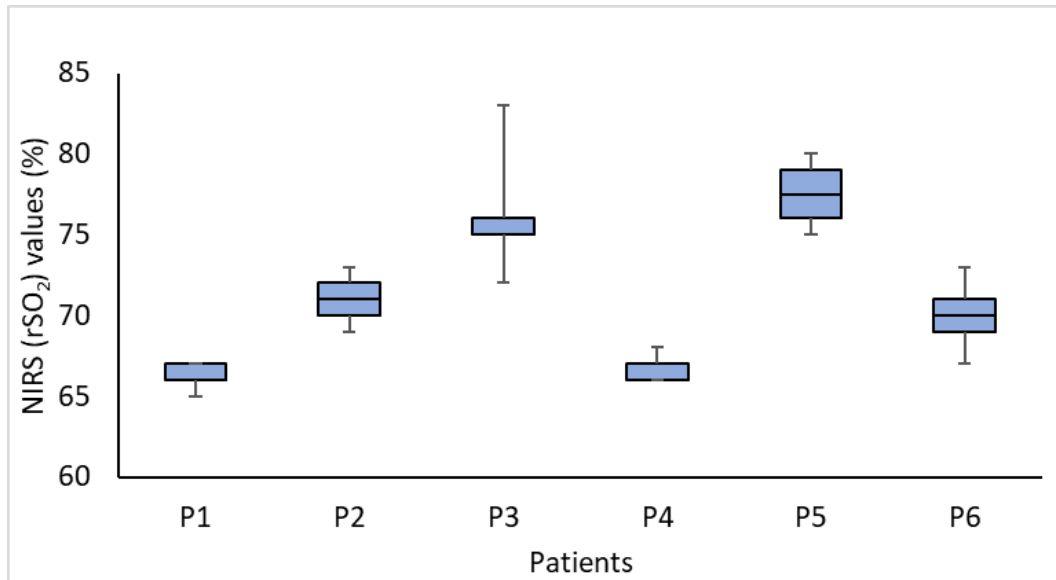
**Graphic 3** - Mean and standard deviation values of HR, SBP, MBP and DBP from T0 until the end of sevoflurane administration. (HR- Heart rate; SBP- Systolic blood pressure; MBP- Mean blood pressure; DBP- Diastolic blood pressure).

When analysing the NIRS values, each patient showed very distinct NIRS trends along the entire study period (graphic 4).



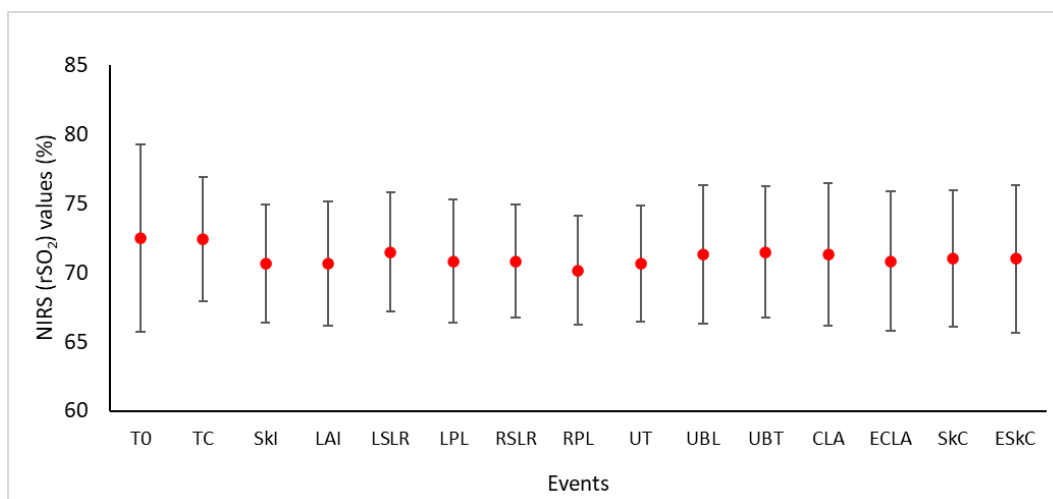
**Graphic 4** - Trend of all NIRS (rSO<sub>2</sub>) values from each patient (P) from T0 until the end of sevoflurane administration. (NIRS- Near infrared spectroscopy; rSO<sub>2</sub>- Regional oxygen saturation).

By observing the graphic 5, the NIRS maximum and minimum values registered per patient, ranged from 83% in patient 3, to 65% in patient 1, respectively. The NIRS values variation within patients is low, except for patient 3.



**Graphic 5** - Boxplot diagram showing median, minimum, and maximum NIRS (rSO<sub>2</sub>) values from each patient from T0 until the end of sevoflurane administration. (NIRS- Near infrared spectroscopy; rSO<sub>2</sub>- Regional oxygen saturation).

The NIRS values at the distinct noxious stimulation can be observed in graphic 6.



**Graphic 6** - Noxious stimuli and the respective NIRS (rSO<sub>2</sub>) values along the sequential surgical events during the anaesthetic procedure. Data are mean ± standard deviation. (T0- five minutes after tracheal intubation; TC- Surgical towel clam; SKI- Skin incision; LAI- Linea alba incision; LSLR- Left suspensory ligament rupture; LPL- Left pedicle ligature; RSLR- Right suspensory



ligament rupture; RPL- Right pedicle ligature; UT- Uterine body traction; UBL- Uterine body ligature; UBT- Uterine body transection; CLA- Closure of the linea alba; ECLA- End closing linea alba; SkC- Skin closure; ESKC- End of skin closure; NIRS- Near infrared spectroscopy; rSO2- Regional oxygen saturation).

From the observation of the mean NIRS values in graphic 6 for each noxious stimulus analysed, the NIRS values remained within 70-75% with a high standard deviation, regardless of the noxious stimuli. No statistically differences were observed at any time point.

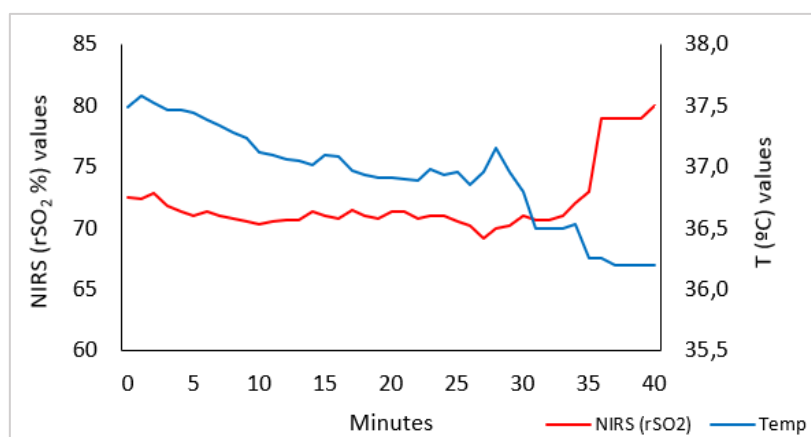
There is a positive correlation between NIRS and MAC (p-value<0.05), HR (p-value<0.01) and SBP (p-value<0.05). A negative correlation was also observed between NIRS and body temperature (p-value<0.05) (table 1).

**Table 1-** Pearson’s (ρ) correlation coefficient and p-values between Near-infrared spectroscopy (NIRS) and sevoflurane minimum alveolar concentration (MAC), body temperature (Temp), heart rate (HR), systolic blood pressure (SBP), diastolic blood pressure (DBP) and mean blood pressure (MBP).

		MAC	Temp.	HR	SBP	DBP	MBP
NIRS	ρ correlation coefficient	0.171	- 0.162	0.213	0.147	- 0.108	0.090
	p-value	0.018*	0.021*	0.001**	0.023*	0.097	0.167

\*p-value<0.05; \*\*p-value<0.01

The graphic 7 shows the NIRS and body temperature mean values from all patients during the study period.



**Graphic 7 -** Mean values of NIRS and body temperature from all patients, during the study period. (NIRS- Near infrared spectroscopy; rSO2- Regional oxygen saturation; T- Body temperature).

## VI. Discussion

This preliminary study addressed the monitoring of the microcirculation using NIRS sensors on the caudal portion of the sartorius muscle, and the NIRS response to noxious stimuli in cats submitted to elective ovariohysterectomy, under anaesthetic premedication with dexmedetomidine, ketamine and methadone, and maintenance of anaesthesia with sevoflurane. The sartorius NIRS range values during the study period were  $71.84 \pm 4.85$  % (65% to 83%). There was a positive correlation between NIRS and sevoflurane MAC (minimum alveolar concentration of volatile anaesthetic required to induce immobilization of 50% of patients exposed to a high noxious stimulus<sup>156-158</sup>), HR, and SBP, and a negative correlation between NIRS and body temperature. NIRS was not able to detect noxious stimulation in cats submitted to ovariohysterectomy under general anaesthesia.

Heart rate, cardiac output and systolic blood pressure work together to assure an adequate tissue perfusion, including the peripheral microcirculatory vessels network that is monitored by NIRS. The amount of blood present in the tissues will influence NIRS values, as peripheral NIRS monitoring is based in continuously real-time measurement of blood haemoglobin oxygen saturation and oxygen balance, that will influence the tissues' haemoglobin concentrations.<sup>3,34,109</sup> Thus, and accordingly to the observations in our study, an increase in heart rate or in systolic blood pressure, under normal physiological conditions, will increase the amount of blood flow that reaches microcirculation per minute. Consequently, this will influence the haemoglobin and oxygen concentrations in the microcirculation, leading to an increase in NIRS values.

Sevoflurane induces a dose-dependent respiratory depression, which increase partial pressure of carbon dioxide ( $\text{PaCO}_2$ ) and, consequently, respiratory acidosis in cats, and a right shifting of the haemoglobin dissociation curve (low affinity of haemoglobin for  $\text{O}_2$ ).<sup>159,160</sup> As, in our study, all cats were mechanically ventilated, and the ventilatory parameters adjusted for maintaining  $\text{SPO}_2$  and  $\text{EtCO}_2$  concentrations within normal physiological values, there was no respiratory depression during the entire study period. Sevoflurane also causes a dose-dependent vasodilation leading to a decrease in systemic vascular resistance, in arterial blood pressure, in cardiac output, and in cardiac inotropism associated with a decrease in the velocity of myocardial relaxation, which may lead to a decrease in oxygen delivery to the tissues.<sup>159,161,162</sup> Thus, a negative correlation between sevoflurane MAC and NIRS values should be expected.

Studies report that sevoflurane can maintain heart rate within physiological normal range values, provide cardiovascular stability with no systemic hemodynamic effects, and preserve  $\text{CO}_2$ -reactivity at 1 MAC of sevoflurane, with a possible ceiling depressing effect in the cardiovascular system of cats at approximately 1.5 MAC.<sup>159,162,163</sup> The cardiovascular and

hemodynamic system remain stable at low sevoflurane MAC values,<sup>162,163</sup> as appeared to have occurred in our study with sevoflurane MAC values ranging from 0.57 MAC to 0.71 MAC, but with a positive correlation between sevoflurane MAC and NIRS values. This positive correlation may suggest that the slight increase in sevoflurane MAC in some patients in our study, could have caused a vasodilation at the microcirculation level,<sup>161,163</sup> which could have changed the normal gas pressures at the microvascular arterial-venous pole,<sup>20,24,164</sup> resulting in a decrease in the O<sub>2</sub> release from oxyhaemoglobin leading to an increased oxyhaemoglobin concentration at the venous pole and, consequently, an increase in muscular NIRS values.<sup>165,166</sup> It can also be speculated that a possible microvascular vasodilation could have resulted in a higher amount of blood in the muscular tissue, that would also lead to an increase in NIRS values.<sup>19</sup>

The negative correlation between body temperature and NIRS reported in our study may be associated with the influence of the temperature variation in the haemoglobin-oxygen affinity.<sup>62</sup> Also, decreasing body temperature in cats below 36.7°C<sup>167,168</sup> causes tissue hypoperfusion, decreasing heart rate and cardiac output, and shifts the intravascular fluid into the tissues, causing haemoconcentration.<sup>169,170</sup> This resulting hypovolemia increases blood viscosity, and low temperatures also decrease cellular energy metabolism and nutrient demands, increase gas solubility and the haemoglobin affinity with oxygen (left shifting of haemoglobin dissociation curve).<sup>169-172</sup> In cats, body temperature values between 36.7°C and 37.7°C are considered mild secondary hypothermia,<sup>173</sup> most commonly associated to surgery and anaesthesia.<sup>174</sup> In our study, cats' temperature during the study period was 37.03±0.12°C (minimum value - 36.2°C; first quartile - 36.5°C; median - 36.9°C; third quartile - 37.5°C; maximum value - 38.2°C) which indicates that the body temperature shifted from normal/near-normal values at the beginning of the study period, to mild secondary hypothermia progressively installed during the anaesthetic and surgical procedure (graphic 7). This decreasing trend in the body temperature would cause changes in the cardiovascular function, as described above, that are the basis for NIRS values to increase. It is important, however, to refer that the negative correlation observed between temperature and NIRS values in this preliminary study should be interpreted with caution. In fact, beyond the 36 minutes of the study period, NIRS and body temperature values were recorded from just one cat (graphics 4 and 7), which could have influenced the correlation results.

Sympathetic nervous system activation affects the hemodynamic system due to neuronal activity, involving changes in blood flow to the different tissues, oxygen consumption, heart rate, blood pressure and, consequently, the concentration of oxygenated and deoxygenated haemoglobin, which is positively correlated with this neuronal activity.<sup>175-177</sup> NIRS evaluate microcirculation and tissues perfusion through the level of haemoglobin's oxygen saturation, and it was hypothesized that NIRS could also reflect the sympathetic response to noxious stimulus at the microcirculation level. Nevertheless, NIRS was not able to detect noxious stimulation in cats submitted to ovariohysterectomy under general anaesthesia with this anesthetic protocol.

## **VII. Conclusion**

The sartorius normal NIRS range values in cats submitted to general anaesthesia for elective ovariohysterectomy procedures is  $71.84 \pm 4.85$  % (65% to 83%). Tissue hypoperfusion should be considered when sartorius NIRS values drop below 62% (two standard deviations below NIRS mean) during general anaesthesia in cats. A positive correlation between NIRS and sevoflurane MAC, HR, and SBP was observed, reflecting the influence of the haemodynamic variables in the sartorius NIRS monitoring values. On the other hand, the negative correlation observed between NIRS and body temperature is interesting because, the haemodynamic changes induced by decreasing temperature values, also reflect a decrease in the metabolic state of the tissue. Which allows us to hypothesize that NIRS technology may have the potential of addressing the tissues' metabolic state. Finally, NIRS was not able to detect noxious stimulation in cats submitted to ovariohysterectomy under general anaesthesia.

The observations from this study reinforce NIRS monitoring as an useful tool for assessing the O<sub>2</sub> tissue saturation, but it is crucial that clinicians interpret NIRS values within a scenario that takes into consideration all the other physiological variables.

## VIII. Bibliography

1. Scholkmann F, Kleiser S, Metz AJ, et al. A review on continuous wave functional near-infrared spectroscopy and imaging instrumentation and methodology. *Neuroimage*. 2014;85:6-27. doi:10.1016/j.neuroimage.2013.05.004
2. Matthes, K., Gross F. Fortlaufende Registrierung der Lichtabsorption des Blutes in zwei verschiedenen Spektralbezirken. *Naunyn Schmiedebergs Arch Pharmacol*. 1938;191((2-4)):381-390.
3. Moerman A, Wouters P. Near-infrared spectroscopy (NIRS) monitoring in contemporary anesthesia and critical care. *Acta Anaesthesiol Belg*. 2010;61(4):185-194.
4. Bouguer P. Essai d'optique, sur la gradation de la lumiere. *Claude Jombert, Paris*. 1729.
5. Beer. Bestimmung der Absorption des rothen Lichts in farbigen Flüssigkeiten. 1852;162(5):78-88. doi:10.1002/andp.18521620505
6. Delpy, D.T., Cope, M., van der Zee, P., Arridge, S., Wray, Susan, and Wyatt J. Estimation of optical pathlength through tissue from direct time of flight measurement. *Phys Med Biol*. 1988;33:1433-1442.
7. Salcedo MC, Tart K, Hall K. A systematic review of human and veterinary applications of noninvasive tissue oxygen monitoring. *J Vet Emerg Crit Care*. 2016;26(3):323-332. doi:10.1111/vec.12465
8. Secomb TW. Hemodynamics. *Compr Physiol*. 2016;6(2):975-1003. doi:10.1002/cphy.c150038
9. Michiels C. Physiological and pathological responses to hypoxia. *Am J Pathol*. 2004;164(6):1875-1882. doi:10.1016/S0002-9440(10)63747-9
10. Ekbal NJ, Dyson A, Black C, Singer M. Monitoring tissue perfusion, oxygenation, and metabolism in critically ill patients. *Chest*. 2013;143(6):1799-1808. doi:10.1378/chest.12-1849
11. Vranken NPA, Weerwind PW. Non-invasive tissue oximetry—an integral puzzle piece. *J Extra Corpor Technol*. 2019;51(3):41-45.

12. Van Beest P, Wietasch G, Scheeren T, Spronk P, Kuiper M. Clinical review: Use of venous oxygen saturations as a goal - a yet unfinished puzzle. *Crit Care*. 2011;15(5):1-9. doi:10.1186/cc10351
13. Boag A. Shock Assessment and Treatment. In: *World Small Animal Veterinary Association World Congress Proceedings*. ; 2015:1-4. <https://www.vin.com/doc/?id=7259440>.
14. Ward KR, Ivatury RR, Barbee RW, et al. Near infrared spectroscopy for evaluation of the trauma patient: A technology review. *Resuscitation*. 2006;68(1):27-44. doi:10.1016/j.resuscitation.2005.06.022
15. Zaleski KL, Kussman BD. Near-Infrared Spectroscopy in Pediatric Congenital Heart Disease. *J Cardiothorac Vasc Anesth*. 2019;34(2):489-500. doi:10.1053/j.jvca.2019.08.048
16. De Backer D. Is microcirculatory assessment ready for regular use in clinical practice? *Curr Opin Crit Care*. 2019;25(3):280-284. doi:10.1097/MCC.0000000000000605
17. Muir W. Trauma: Physiology, pathophysiology, and clinical implications. *J Vet Emerg Crit Care*. 2006;16(4):253-263. doi:10.1111/j.1476-4431.2006.00185.x
18. Mourad JJ, Laville M. Is hypertension a tissue perfusion disorder? Implications for renal and myocardial perfusion. *J Hypertens*. 2006;24(SUPPL. 5):10-16. doi:10.1097/01.hjh.0000240041.43214.8a
19. Magder S. The meaning of blood pressure. *Crit Care*. 2018;22(257):1-10. doi:10.1186/s13054-018-2171-1
20. Jacob M, Chappell D, Becker BF. Regulation of blood flow and volume exchange across the microcirculation. *Crit Care*. 2016;20(1):1-13. doi:10.1186/s13054-016-1485-0
21. Reitsma S, Slaaf DW, Vink H, Van Zandvoort MAMJ, Oude Egbrink MGA. The endothelial glycocalyx: Composition, functions, and visualization. *Pflugers Arch Eur J Physiol*. 2007;454(3):345-359. doi:10.1007/s00424-007-0212-8
22. Cheifetz IM. Cardiorespiratory interactions: The relationship between mechanical ventilation and hemodynamics. *Respir Care*. 2014;59(12):1937-1945. doi:10.4187/respcare.03486

23. Grubb T, Sager J, Analgesia VTSA, et al. 2020 AAHA Anesthesia and Monitoring Guidelines for Dogs and Cats \*. 2020:1-24. doi:10.5326/JAAHA-MS-7055
24. K. Barrett, H. Brooks, S. Boitano SB. *Ganong's Review of Medical Physiology - Section VII: Respiratory Physiology (23rd Edition)*. Vol 4. McGraw-Hil. McGraw-Hill Companies; 2009. doi:10.1111/j.1469-8749.1962.tb03197.x
25. Simmons GH, Minson CT, Cracowski JL, Halliwill JR. Systemic hypoxia causes cutaneous vasodilation in healthy humans. *J Appl Physiol*. 2007;103(2):608-615. doi:10.1152/jappphysiol.01443.2006
26. Yoshimoto S, Ishizaki Y, Sasaki T, Murota SI. Effect of carbon dioxide and oxygen on endothelin production by cultured porcine cerebral endothelial cells. *Stroke*. 1991;22(3):378-383. doi:10.1161/01.STR.22.3.378
27. James M. Walter, Thomas C. Corbridge BDS. Invasive Mechanical Ventilation. *Physiol Behav*. 2018;176(3):139-148. doi:10.1016/j.physbeh.2017.03.040
28. Mahmood SS, Pinsky MR. Heart-lung interactions during mechanical ventilation : the basics. 2018;6(2). doi:10.21037/atm.2018.04.29
29. Young BC, Prittie JE, Fox P, Barton LJ. Decreased central venous oxygen saturation despite normalization of heart rate and blood pressure post shock resuscitation in sick dogs. *J Vet Emerg Crit Care*. 2014;24(2):154-161. doi:10.1111/vec.12154
30. Scheeren TWL, Schober P, Schwarte LA. Monitoring tissue oxygenation by near infrared spectroscopy (NIRS): Background and current applications. *J Clin Monit Comput*. 2012;26(4):279-287. doi:10.1007/s10877-012-9348-y
31. Benedik PS. Monitoring Tissue Blood Flow and Oxygenation. A Brief Review of Emerging Techniques. *Crit Care Nurs Clin North Am*. 2014;26(3):345-356. doi:10.1016/j.ccell.2014.04.003
32. Perutz M. Hoppe-Seyler, Stokes and Haemoglobin. *Biol Chem Hoppe Seyler*. 1995;376(8):449-450. doi:10.1515/bchm3.1995.376.8.449
33. von Vierordt K. Die quantitative Spectralanalyse in ihrer Anwendung auf Physiologie, Physik, Chemie und Technologie. 1876. doi:10.1002/ardp.18762090157

34. Hamaoka T, McCully KK. Review of early development of near-infrared spectroscopy and recent advancement of studies on muscle oxygenation and oxidative metabolism. *J Physiol Sci.* 2019;69(6):799-811. doi:10.1007/s12576-019-00697-2
35. Hüfner G. Neue Versuche zur Bestimmung der Sauerstoffcapazität des Blutfarbstoffs. *Arch Pathol Anat Physiol Klin Med.* 1894;55:130–176.
36. Matthes, K., Gross F. Fortlaufende Registrierung der Lichtabsorption der Farbe des Blutes in zwei verschiedenen Spektralbezirken. *Arch Exp Pathol Pharmacol.* 1939;191:381-390.
37. Jobsis FF. Noninvasive infrared monitoring of cerebral and myocardial oxygen sufficiency and circulatory parameters. *Science (80- ).* 1977;198:1264-1267.
38. Schwarz G, Litscher G, Kleinert R, Jobstmann R. Cerebral oximetry in dead subjects. *J Neurosurg Anesthesiol.* 1996;8(3):189-193. doi:10.1097/00008506-199607000-00001
39. Litscher, G., Schwarz G. Transcranial Cerebral Oximetry - is it clinically useless at this moment to interpret absolute values obtained by INVOS 3100 cerebral oximeter? *Biomed Tech.* 1997;42:74-77. doi:10.1097/00008506-199807000-00021
40. Strangman G, Boas DA, Sutton JP. Non-invasive neuroimaging using near-infrared light. *Biol Psychiatry.* 2002;52(7):679-693. doi:10.1016/S0006-3223(02)01550-0
41. Hiwatashi K, Doi K, Mizuno R, Yokosuka M. Examiner's finger-mounted near-infrared spectroscopy is feasible to analyze cerebral and skeletal muscle oxygenation in conscious Chihuahuas. *J Biomed Opt.* 2017;22(2):026006. doi:10.1117/1.jbo.22.2.026006
42. Wahr J. A., Tremper K.K., Samra S. DDT. Near-infrared Spectroscopy: Theory and Applications. *J Cardiothorac Vasc Anesth.* 1996;10(3):406-418.
43. Currà A, Gasbarrone R, Cardillo A, et al. Near-infrared spectroscopy as a tool for in vivo analysis of human muscles. *Sci Rep.* 2019;(November 2018):1-14. doi:10.1038/s41598-019-44896-8
44. D'Amico A, Natale C Di, Castro F Lo, Iarossi S, Catini A, Martinelli E. Volatile compounds detection by IR acousto-optic detectors. *NATO Sci Peace Secur Ser B Phys Biophys.* 2009:21-59. doi:10.1007/978-1-4020-9253-4-2
45. Roggan, A., Dorschel, K., Minet, O., Wolff, D., Müller G. The optical properties of biological



- tissue in the near-infrared wavelength range - review and measurements. In: Roggan, A., Muller G, ed. *Laser-Induced Interstitial Thermotherapy, Part II: Optical and Thermal Properties of Biological Tissue*. Bellingham, Washington USA: SPIE - The international society for optical engineering; 1995:10-44.
46. Davidovits P. *Physics in Biology and Medicine (16.2-Spectroscopy)*. Vol 9. third edit. Academic Press is a imprint of Elsevier; 2008.
  47. Zhang JXJ, Hoshino K. Optical transducers: Optical molecular sensing and spectroscopy. In: *Molecular Sensors and Nanodevices*. ; 2019:231-309. doi:10.1016/b978-0-12-814862-4.00005-3
  48. Bakker A, Smith B, Ainslie P, Smith K. Near-Infrared Spectroscopy. In: *Applied Aspects of Ultrasonography in Humans*. Vol 74. InTech; 2012:65-88. doi:10.5772/32493
  49. Boezeman RPE, Moll FL, Ünlü Ç, de Vries JPPM. Systematic review of clinical applications of monitoring muscle tissue oxygenation with near-infrared spectroscopy in vascular disease. *Microvasc Res*. 2016;104:11-22. doi:10.1016/j.mvr.2015.11.004
  50. Delpy DT, Cope M. Quantification in tissue near-infrared spectroscopy. *Philos Trans R Soc B Biol Sci*. 1997;352(1354):649-659. doi:10.1098/rstb.1997.0046
  51. Ferrari M., Mottola L. Q V. Principles, techniques, and limitations of near infrared spectroscopy. *Can J Appl Physiol*. 2004;29(August 2004).
  52. Rasulo F., Matta B VN. *Cerebral Blood Flow Monitoring*. Elsevier Inc.; 2018. doi:10.1016/B978-0-12-809915-5.00002-4
  53. Baker WB, Parthasarathy AB, Busch DR, Mesquita RC, Greenberg JH, Yodh AG. Modified Beer-Lambert law for blood flow. *Biomed Opt Express*. 2014;5(11):4053. doi:10.1364/boe.5.004053
  54. Sassaroli A, Fantini S. Comment on the modified Beer-Lambert law for scattering media. *Phys Med Biol*. 2004;49(14). doi:10.1088/0031-9155/49/14/N07
  55. Bhatt M, Ayyalasomayajula KR, Yalavarthy PK. Generalized Beer-Lambert model for near-infrared light propagation in thick biological tissues. *J Biomed Opt*. 2016;21(7):076012. doi:10.1117/1.jbo.21.7.076012

56. Valipour A, McGown AD, Makker H, O'Sullivan C, Spiro SG. Some factors affecting cerebral tissue saturation during obstructive sleep apnoea. *Eur Respir J*. 2002;20(2):444-450. doi:10.1183/09031936.02.00265702
57. Igne B, Talwar S, Feng H, Drennen JK, Anderson CA. Near-Infrared Spatially Resolved Spectroscopy for Tablet Quality Determination. *J Pharm Sci*. 2015;104(12):4074-4081. doi:10.1002/jps.24618
58. Kovacsova, Z., Bale, G., Mitra, S., De Roever, I., Meek, J., Robertson, N., Tachtsidis I. Investigation of Confounding Factors in Measuring Tissue Saturation with NIRS Spatially Resolved Spectroscopy. *Oxyg Transp to Tissue XL, Adv Exp Med Biol 1072*. 2018:307-312. doi:10.1007/978-3-319-91287-5
59. León-Carrión J, León-Domínguez U. Functional Near-Infrared Spectroscopy (fNIRS): Principles and Neuroscientific Applications. *Neuroimaging - Methods*. 2012;(January 2012). doi:10.5772/23146
60. Mairbäurl H, Weber RE. Oxygen transport by hemoglobin. *Compr Physiol*. 2012;2(2):1463-1489. doi:10.1002/cphy.c080113
61. Gell DA. Structure and function of haemoglobins. *Blood Cells, Mol Dis*. 2018;70(May 2017):13-42. doi:10.1016/j.bcmd.2017.10.006
62. Yuan Y, Shen TJ, Gupta P, et al. A biochemical-biophysical study of hemoglobins from woolly mammoth, asian elephant, and humans. *Biochemistry*. 2011;50(34):7350-7360. doi:10.1021/bi200777j
63. Coletta M, Angeletti M, Ascone I, et al. Heterotropic Effectors Exert More Significant Strain on Monoligated than on Unligated Hemoglobin. *Biophys J*. 1999;76(3):1532-1536. doi:10.1016/S0006-3495(99)77312-1
64. Li Y, Park JS, Deng JH, Bai Y. Cytochrome c oxidase subunit IV is essential for assembly and respiratory function of the enzyme complex. *J Bioenerg Biomembr*. 2006;38(5-6):283-291. doi:10.1007/s10863-006-9052-z
65. Holper L, Lan MJ, Brown PJ, Sublette EM, Burke A, Mann JJ. Brain cytochrome-c-oxidase as a marker of mitochondrial function: A pilot study in major depression using NIRS. *Depress Anxiety*. 2019;36(8):766-779. doi:10.1002/da.22913

66. de Roever, I., Bale, G., Cooper, R.J., Tachtsidis I. Functional NIRS Measurement of Cytochrome-C-Oxidase Demonstrates a More Brain-Specific Marker of Frontal Lobe Activation Compared to the Haemoglobins Isabel. *Oxyg Transp to Tissue XXXIX, Adv Exp Med Biol* 977, capther 19. 2017;977:141-147. doi:10.1007/978-3-319-55231-6
67. Lange, F., Dunne, L., Tachtsidis I. Evaluation of haemoglobin and cytochrome responses during forearm ischaemia using multi-wavelength time domain NIRS. *Oxyg Transp to Tissue XXXIX, Adv Exp Med Biol Chapter 10*. 2017;977:67-72. doi:10.1007/978-3-319-55231-6
68. Mitra S, Bale G, Meek J, Tachtsidis I. Cerebral Near Infrared Spectroscopy Monitoring in Term Infants With Hypoxic Ischemic Encephalopathy — A Systematic Review. 2020;11(May). doi:10.3389/fneur.2020.00393
69. Gunner MR, Amin M, Zhu X, Lu J. Molecular mechanisms for generating transmembrane proton gradients. *Biochim Biophys Acta - Bioenerg.* 2013;1827(8-9):892-913. doi:10.1016/j.bbabbio.2013.03.001
70. Banaji M., Mallet A., Elwell C.E., Nicholls P., Tachtsidis I., Smith M. CCE. Modelling of Mitochondrial Oxygen Consumption and NIRS Detection of Cytochrome Oxidase Redox State. *Adv Exp Med Biol*. 2010;662:285-291. doi:10.1007/978-1-4419-1241-1
71. Mason MG, Nicholls P, Cooper CE. Re-evaluation of the near infrared spectra of mitochondrial cytochrome c oxidase: Implications for non invasive in vivo monitoring of tissues. *Biochim Biophys Acta - Bioenerg.* 2014;1837(11):1882-1891. doi:10.1016/j.bbabbio.2014.08.005
72. Lingzhong Meng, Shaun E. Gruenbaum, Feng Dai TW. Physiology, intervention, and outcomes: three critical questions about cerebral tissue oxygen saturation monitoring. 2018;84(5):599-614. doi:10.23736/S0375-9393.18.12476-X
73. Ghanayem NS, Hoffman GM. Near infrared spectroscopy as a hemodynamic monitor in critical illness. *Pediatr Crit Care Med.* 2016;17(8):S201-S206. doi:10.1097/PCC.0000000000000780
74. Ferrari M, Quaresima V. A brief review on the history of human functional near-infrared spectroscopy (fNIRS) development and fields of application. *Neuroimage.* 2012;63(2):921-935. doi:10.1016/j.neuroimage.2012.03.049

75. Van Essen T, Goos TG, Van Ballegooijen L, et al. Comparison of frequency-domain and continuous-wave near-infrared spectroscopy devices during the immediate transition. *BMC Pediatr.* 2020;20(1):1-9. doi:10.1186/s12887-020-1987-4
76. Davies DJ, Clancy M, Lighter D, et al. Frequency-domain vs continuous-wave near-infrared spectroscopy devices: a comparison of clinically viable monitors in controlled hypoxia. *J Clin Monit Comput.* 2016;31(5):967-974. doi:10.1007/s10877-016-9942-5
77. Lange F, Dunne L, Hale L, Tachtsidis I. MAESTROS: A Multiwavelength Time-Domain NIRS System to Monitor Changes in Oxygenation and Oxidation State of Cytochrome-C-Oxidase. *IEEE J Sel Top Quantum Electron.* 2019;25(1). doi:10.1109/JSTQE.2018.2833205
78. Sudakou A, Wojtkiewicz S, Lange F, et al. Depth-resolved assessment of changes in concentration of chromophores using time-resolved near-infrared spectroscopy: estimation of cytochrome-c-oxidase uncertainty by Monte Carlo simulations. *Biomed Opt Express.* 2019;10(9):4621. doi:10.1364/boe.10.004621
79. Wong FY, Alexiou T, Samarasinghe T, Brodecky V, Walker AM. Cerebral arterial and venous contribution to tissue oxygenation Index measured using Spatially Resolved Spectroscopy in Newborn Lambs. *Am Soc Anesthesiol.* 2010;113(6):1385-1391.
80. Veesa JD, Dehghani H. Functional near infrared spectroscopy using spatially resolved data to account for tissue scattering: A numerical study and arm-cuff experiment. *J Biophotonics.* 2019;12(10):1-11. doi:10.1002/jbio.201900064
81. Al-rawi PG, Smielewski P, Hobbiger H, Ghosh S, Kirkpatrick PJ. Assessment of Spatially Resolved Spectroscopy during cardiopulmonary bypass. *J Biomed Opt.* 1999;4(2):208-216.
82. Durduran T, Yodh AG. Diffuse correlation spectroscopy for non-invasive, micro-vascular cerebral blood flow measurement. *Neuroimage.* 2014;85:51. doi:10.1016/j.neuroimage.2013.06.017
83. Carp SA, Farzam P, Redes N, Hueber DM, Franceschini MA. Combined multi-distance frequency domain and diffuse correlation spectroscopy system with simultaneous data acquisition and real-time analysis. *Biomed Opt Express.* 2017;8(9):3993. doi:10.1364/boe.8.003993

84. Karthikeyan P, Moradi S, Ferdinando H, Zhao Z, Myllylä T. Optics based label-free techniques and applications in brain monitoring. *Appl Sci.* 2020;10(6). doi:10.3390/app10062196
85. Wilcox T, Biondi M. fNIRS in the developmental sciences. 2015;6(June). doi:10.1002/wcs.1343
86. Kim HY, Seo K, Jeon HJ, Lee U, Lee H. Application of functional near-infrared spectroscopy to the study of brain function in humans and animal models. *Mol Cells.* 2017;40(8):523-532. doi:10.14348/molcells.2017.0153
87. von Lümann A. openNIRS Documentation. *www.openNIRS.org*, excerpt Master's Thesis "Design Eval a Syst Mob Brain Act Meas using Funct Near-Infrared Spectrosc. 2014.
88. Sutoko S, Sato H, Maki A, et al. Tutorial on platform for optical topography analysis tools. *Neurophotonics.* 2016;3(1):010801. doi:10.1117/1.nph.3.1.010801
89. Lee CW, Cooper RJ, Austin T. Diffuse optical tomography to investigate the newborn brain. *Pediatr Res.* 2017;82(3):376-386. doi:10.1038/pr.2017.107
90. Murkin JM, Arango M. Near-infrared spectroscopy as an index of brain and tissue oxygenation. *Br J Anaesth.* 2009;103(SUPPL.1):3-13. doi:10.1093/bja/aep299
91. Denault A, Shaaban Ali M, Couture EJ, et al. A Practical Approach to Cerebro-Somatic Near-Infrared Spectroscopy and Whole-Body Ultrasound. *J Cardiothorac Vasc Anesth.* 2019;33:S11-S37. doi:10.1053/j.jvca.2019.03.039
92. Kamran MA, Mannann MMN, Jeong MY. Differential path-length factor's effect on the characterization of brain's hemodynamic response function: A functional near-infrared study. *Front Neuroinform.* 2018;12(June):1-15. doi:10.3389/fninf.2018.00037
93. Mcconnell EJ, Rioja E, Bester L, Sanz MG, Fosgate GT, Saulez MN. Use of near-infrared spectroscopy to identify trends in regional cerebral oxygen saturation in horses. *Equine Vet J.* 2012;45(4):470-475. doi:10.1111/evj.12001
94. Gygax L, Reefmann N, Pilheden T, Scholkmann F, Keeling L. Dog behavior but not frontal brain reaction changes in repeated positive interactions with a human: A non-invasive pilot study using functional near-infrared spectroscopy (fNIRS). *Behav Brain Res.*

2014;281:172-176. doi:10.1016/j.bbr.2014.11.044

95. Hou X, Ding H, Teng Y, Zhou C, Tang X. Research on the relationship between brain anoxia at different regional oxygen saturations and brain damage using near-infrared spectroscopy. *Physiol Meas*. 2007;28:1251-1265. doi:10.1088/0967-3334/28/10/010
96. Hazle MA, Gajarski RJ, Aiyagari R, et al. Urinary biomarkers and renal near-infrared spectroscopy predict intensive care unit outcomes after cardiac surgery in infants younger than 6 months of age. *J Thorac Cardiovasc Surg*. 2013;146(4):861-867.e1. doi:10.1016/j.jtcvs.2012.12.012
97. Malakasioti G, Marks SD, Watson T, et al. Continuous monitoring of kidney transplant perfusion with near-infrared spectroscopy. 2018;(May):1-7. doi:10.1093/ndt/gfy116
98. Schat TE, Schurink M, Van Der Laan ME, et al. Near-infrared spectroscopy to predict the course of necrotizing enterocolitis. *PLoS One*. 2016;11(5):1-14. doi:10.1371/journal.pone.0154710
99. Seager E, Longley C, Aladangady N, Banerjee J. Measurement of gut oxygenation in the neonatal population using near-infrared spectroscopy: A clinical tool? *Arch Dis Child Fetal Neonatal Ed*. 2019;105(1):F76-F86. doi:10.1136/archdischild-2018-316750
100. Gay AN, Lazar DA, Stoll B, et al. Near-infrared spectroscopy measurement of abdominal tissue oxygenation is a useful indicator of intestinal blood flow and necrotizing enterocolitis in premature piglets. *J Pediatr Surg*. 2011;46(6):1034-1040. doi:10.1016/j.jpedsurg.2011.03.025
101. Martini S, Corvaglia L. Splanchnic NIRS monitoring in neonatal care: Rationale, current applications and future perspectives. *J Perinatol*. 2018;38(5):431-443. doi:10.1038/s41372-018-0075-1
102. Nahum E, Pw S, Re G, Aj M, Ed S. Correlation of transcutaneous hepatic near- infrared spectroscopy readings with liver surface readings and perfusion parameters in a piglet endotoxemic shock model. *Liver Int*. 2006;26:1277-1282. doi:10.1111/j.1478-3231.2006.01383.x
103. Kaufman, J., Almodovar, M. C., Zuk, J., Friesen RH. Correlation of abdominal site near-infrared spectroscopy with gastric tonometry in infants following surgery for congenital

- heart disease\*. *Pediatr Crit Care Med.* 2008;9(1). doi:10.1097/01.PCC.0000298640.47574.DA
104. Aydogdu O, Burgu B, Gocun PU, et al. Near Infrared Spectroscopy to Diagnose Experimental Testicular Torsion: Comparison With Doppler Ultrasound and Immunohistochemical Correlation of Tissue Oxygenation and Viability. *JURO.* 2012;187(2):744-750. doi:10.1016/j.juro.2011.09.145
  105. Walton RAL, Hansen BD. Venous oxygen saturation in critical illness. *J Vet Emerg Crit Care.* 2018;28(5):387-397. doi:10.1111/vec.12749
  106. Samraj RS, Kerrigan M, Mejia M, et al. Thenar Muscle Oxygen Saturation Levels: A Surrogate for Central Venous Oxygen Saturation? *Clin Pediatr (Phila).* 2019;58(5):528-533. doi:10.1177/0009922819832094
  107. Lima A, van Bommel J, Jansen TC, Ince C, Bakker J. Low tissue oxygen saturation at the end of early goal-directed therapy is associated with worse outcome in critically ill patients. *Crit Care.* 2009;13 Suppl 5:1-7. doi:10.1186/cc8011
  108. Perrey S, Ferrari M. Muscle Oximetry in Sports Science: A Systematic Review. *Sport Med.* 2018;48(3):597-616. doi:10.1007/s40279-017-0820-1
  109. Benni PB, MacLeod D, Ikeda K, Lin HM. A validation method for near-infrared spectroscopy based tissue oximeters for cerebral and somatic tissue oxygen saturation measurements. *J Clin Monit Comput.* 2018;32(2):269-284. doi:10.1007/s10877-017-0015-1
  110. Hamaoka T, Katsumura T, Murase N, et al. Quantification of ischemic muscle deoxygenation by near infrared time-resolved spectroscopy. *J Biomed Opt.* 2000;5(1):102. doi:10.1117/1.429975
  111. Yoxall CW, Weindling AM. Measurement of venous oxyhaemoglobin saturation in the adult human forearm by near infrared spectroscopy with venous occlusion. *Med Biol Eng Comput.* 1997;35(4):331-336. doi:10.1007/BF02534086
  112. Wilson JR, Mancini DM, McCully K, Ferraro N, Lanoce V, Chance B. Noninvasive detection of skeletal muscle underperfusion with near-infrared spectroscopy in patients with heart failure. *Circulation.* 1989;80(6):1668-1674. doi:10.1161/01.CIR.80.6.1668

113. Pavlisko ND, Henao-Guerrero N, Killos MB, et al. Evaluation of tissue oxygen saturation with near-infrared spectroscopy during experimental acute hemorrhagic shock and resuscitation in dogs. *Am J Vet Res.* 2014;75(1):48-53. doi:10.2460/ajvr.75.1.48
114. Taylor JH, Mulier KE, Myers DE, Beilman GJ. Use of near-infrared spectroscopy in early determination of irreversible hemorrhagic shock. *J Trauma - Inj Infect Crit Care.* 2005;58(6):1119-1125. doi:10.1097/01.TA.0000169951.20802.20
115. Pang CCY. Measurement of body venous tone. *J Pharmacol Toxicol Methods.* 2000;44(2):341-360. doi:10.1016/S1056-8719(00)00124-6
116. Jobsis-vanderVliet FF. Discovery of the Near-infrared window into the body and the early development of Near-infrared spectroscopy. *J Biomed Opt.* 1999;4(4):392-396.
117. Piantadosi CA, Jöbsis-Vander Vliet FF. Near infrared optical monitoring of intact skeletal muscle during hypoxia and hemorrhagic hypotension in cats. *Adv Exp Med Biol.* 1985;191:855-862. doi:10.1007/978-1-4684-3291-6\_86
118. Hamaoka T, McCully KK, Quaresima V, Yamamoto K, Chance B. Near-infrared spectroscopy/imaging for monitoring muscle oxygenation and oxidative metabolism in healthy and diseased humans. *J Biomed Opt.* 2007;12(6):062105. doi:10.1117/1.2805437
119. Ferrari M, Muthalib M, Quaresima V. The use of near-infrared spectroscopy in understanding skeletal muscle physiology: Recent developments. *Philos Trans R Soc A Math Phys Eng Sci.* 2011;369(1955):4577-4590. doi:10.1098/rsta.2011.0230
120. Rhee P, Langdale L, Mock C, Gentilello LM. Near-infrared spectroscopy: Continuous measurement of cytochrome oxidation during hemorrhagic shock. *Crit Care Med.* 1997;25(1):166-170. doi:10.1097/00003246-199701000-00030
121. Beilman GJ, Blondet JJ. Near-infrared spectroscopy-derived tissue oxygen saturation in battlefield injuries: A case series report. *World J Emerg Surg.* 2009;4(1):1-7. doi:10.1186/1749-7922-4-25
122. Gingold BM, Killos MB, Griffith E, Posner L. Measurement of peripheral muscle oxygen saturation in conscious healthy horses using a near-infrared spectroscopy device. *Vet Anaesth Analg.* 2019;46(6):789-795. doi:10.1016/j.vaa.2019.07.001



123. Hall KE, Powell LL, Beilman GJ, Shafer KR, Skala VK, Olmstead EA. Measurement of tissue oxygen saturation levels using portable near-infrared spectroscopy in clinically healthy dogs. *J Vet Emerg Crit Care*. 2008;18(6):594-600. doi:10.1111/j.1476-4431.2008.00369.x
124. Engbers S, Boysen SR, Engbers J, Chalhoub S. A comparison of tissue oxygen saturation measurements by 2 different near-infrared spectroscopy monitors in 21 healthy dogs. *J Vet Emerg Crit Care*. 2014;24(5):536-544. doi:10.1111/vec.12229
125. Buckland, A., Pan, W.R., Dhar, S., Edwards, G., Rozen, W.M., Ashton, M.W., Taylor GI. Neurovascular Anatomy of Sartorius Muscle Flaps: Implications for Local Transposition and Facial Reanimation. *Am Soc Plast Surg*. 2008;123:44-54. doi:10.1097/PRS.0b013e3181904bc6
126. Boushel R, Piantadosi CA. Near-infrared spectroscopy for monitoring muscle oxygenation. *Acta Physiol Scand*. 2000;168(4):615-622. doi:10.1046/j.1365-201X.2000.00713.x
127. Hampson NB, Piantadosi CA. Near-infrared optical responses in feline brain and skeletal muscle tissues during respiratory acid-base imbalance. *Brain Res*. 1990;519(1-2):249-254. doi:10.1016/0006-8993(90)90085-P
128. Shahar R, Milgram J. Morphometric and anatomic study of the hind limb of a dog. *Am J Vet Res*. 2001;62(6). doi:10.2460/ajvr.2001.62.928
129. Ghoshall NG. The Arteries of the Pelvic Limb of the Cat ( *Felis domesticus* ). 1972;19:78-85. doi:10.1111/j.1439-0442.1972.tb00295.x
130. Sacks, Robert D., and Roy RR. Architecture of the Hind Limb Muscles of Cats : Functional Significance. *J Morphol*. 1982:185-195.
131. Epstein CD, Haghenbeck KT. Bedside assessment of tissue oxygen saturation monitoring in critically ill adults: An integrative review of the literature. *Crit Care Res Pract*. 2014;2014. doi:10.1155/2014/709683
132. Sullivan LA, Campbell VL, Radecki S V., Webb CB. Comparison of tissue oxygen saturation in ovariohysterectomized dogs recovering on room air versus nasal oxygen insufflation. *J Vet Emerg Crit Care*. 2011;21(6):633-638. doi:10.1111/j.1476-4431.2011.00693.x

133. Myers D, McGraw M, George M, Mulier K, Beilman G. Tissue hemoglobin index: A non-invasive optical measure of total tissue hemoglobin. *Crit Care*. 2009;13(SUPPL. 5). doi:10.1186/cc8000
134. Karahan MA, Binici O, Büyükfırat E. Tissue oxygen saturation change on upper extremities after ultrasound-guided infraclavicular brachial plexus blockade; prospective observational study. *Med*. 2019;55(6). doi:10.3390/medicina55060274
135. Uchida T, Kanayama N, Kawai K, Niwayama M. Craniofacial tissue oxygen saturation is associated with blood pH using an examiner's finger-mounted tissue oximetry in mice. *J Biomed Opt*. 2016;21(4):040502. doi:10.1117/1.jbo.21.4.040502
136. Proctor, H.J., Palladino, G.W., Fillipo D. Failure of autoregulation after closed head injury: an experimental model. *J Trauma*. 1988;28:347-352.
137. Cairns, Charles B., Fillipo, Drew, Palladino, G. William, and Proctor HJ. Direct Noninvasive Assessment of Brain Metabolism during Increased Intracranial Pressure: Potential Therapeutic Vistas. *J Trauma*. 1986;26(10):863-868.
138. Mook, P.H., Proctor, H.J., Jobsis, F., Wildevuur CR. Assessment of brain oxygenation : a comparison between an oxygen electrode and near-infrared spectrophotometry. *Adv Exp Med Biol*. 1984. doi:10.1007/978-1-4684-1188-1
139. Wada H, Watari M, Sueda T, et al. Cerebral tissue oxygen saturation during percutaneous cardiopulmonary support in a canine model of respiratory failure. *Artif Organs*. 2000;24(8):640-643. doi:10.1046/j.1525-1594.2000.06601.x
140. Newton CRJC, Wilson DA, Gunnoe E, Wagner B, Cope M, Traystman RJ. Measurement of cerebral blood flow in dogs with near infrared spectroscopy in the reflectance mode is invalid. *J Cereb Blood Flow Metab*. 1997;17(6):695-703. doi:10.1097/00004647-199706000-00011
141. Silva A, Venâncio C, Ortiz AL, Souza AP, Amorim P, Ferreira DA. The effect of high doses of remifentanil in brain near-infrared spectroscopy and in electroencephalographic parameters in pigs. *Vet Anaesth Analg*. 2014;41(2):153-162. doi:10.1111/vaa.12091
142. Oya S, Inoue H, Nakade T, Ogata A, Tamura M, Kato S. Near-infrared spectroscopy evaluated as a technique for estimating udder haemodynamics in the lactating cow. *J Vet*

*Med Ser A Physiol Pathol Clin Med.* 2003;50(5):230-234. doi:10.1046/j.1439-0442.2003.00524.x

143. Zaidi AD, Munk MHJ, Schmidt A, et al. Simultaneous epidural functional Near-InfraRed Spectroscopy and cortical electrophysiology as a tool for studying local neuro-vascular coupling in primates. *Neuroimage.* 2015. doi:10.1016/j.neuroimage.2015.07.019
144. Wakita M, Shibasaki M, Ishizuka T, Schnackenberg J, Fujiawara M, Masataka N. Measurement of neuronal activity in a macaque monkey in response to animate images using near-infrared spectroscopy. 2010;4(June):1-8. doi:10.3389/fnbeh.2010.00031
145. Lee Y, Pollet V, Kato A, Goto Y. Prefrontal cortical activity associated with visual stimulus categorization in non-human primates measured with near-infrared spectroscopy. *Behav Brain Res.* 2017;317:327-331. doi:10.1016/j.bbr.2016.09.068
146. Fuster, Joaquín, Guiou, Michael, Ardestani, Allen, Cannestra, Andrew, Sheth, Sameer, Zhou, Yong-Di, Toga, Arthur, and Bodner M. Near-infrared spectroscopy ( NIRS ) in cognitive neuroscience of the primate brain. 2005;26:215-220. doi:10.1016/j.neuroimage.2005.01.055
147. Ardestani A, Shen W, Darvas F, Toga AW, Fuster JM. Modulation of Frontoparietal Neurovascular Dynamics in Working Memory. 2015:1-23. doi:10.1162/jocn
148. Guldemann K, Vögeli S, Wolf M, Wechsler B, Gyax L. Brain and Cognition Frontal brain deactivation during a non-verbal cognitive judgement bias test in sheep. *BRAIN Cogn.* 2015;93:35-41. doi:10.1016/j.bandc.2014.11.004
149. Vögeli S, Lutz J, Wolf M, Wechsler B, Gyax L. Valence of physical stimuli , not housing conditions , affects behaviour and frontal cortical brain activity in sheep. *Behav Brain Res.* 2014;267:144-155. doi:10.1016/j.bbr.2014.03.036
150. Vögeli, Sabine, Wolf, Martin, Wechsler, Beat, Gyax L. Frontal brain activity and behavioral indicators of affective states are weakly affected by thermal stimuli in sheep living in different housing. *Front Vet Sci.* 2015;2:1-10. doi:10.3389/fvets.2015.00009
151. Muehleman T, Reefmann N, Wechsler B, Wolf M, Gyax L. NeuroImage In vivo functional near-infrared spectroscopy measures mood-modulated cerebral responses to a positive emotional stimulus in sheep. *Neuroimage.* 2011;54(2):1625-1633.

doi:10.1016/j.neuroimage.2010.08.079

152. Gygax L, Reefmann N, Wolf M, Langbein J. Prefrontal cortex activity , sympatho-vagal reaction and behaviour distinguish between situations of feed reward and frustration in dwarf goats. *Behav Brain Res*. 2013;239:104-114. doi:10.1016/j.bbr.2012.10.052
153. McKnight JC, Bennett KA, Bronkhorst M, et al. Shining new light on mammalian diving physiology using wearable near-infrared spectroscopy. *PLoS Biol*. 2019;17(6):1-20. doi:10.1371/journal.pbio.3000306
154. Doi K, Hiwatashi K, Yokosuka M, Mizuno R. A near - infrared spectroscopy ( NIRS ) device unveils oxygenation levels in skeletal muscle and brain of a conscious Harris ' s Hawk ( *Parabuteo unicinctus* ). *J Ornithol*. 2020:3-6. doi:10.1007/s10336-020-01784-7
155. Redford D, Paidy S, Kashif F. Absolute and Trend Accuracy of a New Regional Oximeter in Healthy Volunteers During Controlled Hypoxia. *Int Anesth Res Soc*. 2014;119(6):1315-1319. doi:10.1213/ANE.0000000000000474
156. Shaughnessy MR, Hofmeister EH. A systematic review of sevoflurane and isoflurane minimum alveolar concentration in domestic cats. *Vet Anaesth Analg*. 2014;41(1):1-13. doi:10.1111/vaa.12083
157. Lobo, Sharlene A.; Lopez J. Minimum alveolar concentration (MAC). 2020.
158. Natalini CC. Sevoflurane, Desflurane, and Xenon New Inhaled Anesthetics in Veterinary Medicine. *Ciência Rural*. 2001;31(1):177-183. doi:10.1590/s0103-84782001000100029
159. Pypendop BH, Ilkiw JE. Hemodynamic effects of sevoflurane in cats. *Am J Vet Res*. 2004;65(1):20-25. doi:10.2460/ajvr.2004.65.20
160. Hikasa Y, Yamashita M, Takase K, Ogasawara S. Prolonged Sevoflurane, Isoflurane and Halothane Anaesthesia in Oxygen Using Rebreathing or Non-rebreathing System in Cats. *J Vet Med Ser A Physiol Pathol Clin Med*. 1998;45(9):559-575. doi:10.1111/j.1439-0442.1998.tb00860.x
161. Michailidou A, Trenz H-J, de Wilde P. Annex I: Summary of product characteristics - SevoFlo 100%. *Internet Eur Integr*. 2019:167-172. doi:10.2307/j.ctvdf0dxq.12
162. Souza AP, Henao Guerrero PN, Nishimori CT, et al. Cardiopulmonary and acid-base

- effects of desflurane and sevoflurane in spontaneously breathing cats. *J Feline Med Surg.* 2005;7(2):95-100. doi:10.1016/j.jfms.2004.06.003
163. Juhász M, Molnár L, Fülesdi B, Végh T, Páll D, Molnár C. Effect of sevoflurane on systemic and cerebral circulation, cerebral autoregulation and CO<sub>2</sub> reactivity. *BMC Anesthesiol.* 2019;19(1):1-8. doi:10.1186/s12871-019-0784-9
  164. Broome IJ, Mills GH, Spiers P, Reilly CS. An evaluation of the effect of vasodilatation on oxygen saturations measured by pulse oximetry and venous blood gas analysis. *Anaesthesia.* 1993;48(5):415-416. doi:10.1111/j.1365-2044.1993.tb07017.x
  165. Higgins C. Oxygen saturation – better measured than calculated. 2014:1-7.
  166. Patel S, Mohiuddin SS. Physiology, Oxygen Transport And Carbon Dioxide Dissociation Curve. *StatPearls.* 2020. <http://www.ncbi.nlm.nih.gov/pubmed/30969637>.
  167. Grubb T, Sager J, Gaynor JS, et al. 2020 AAHA Anesthesia and Monitoring Guidelines for Dogs and Cats. *J Am Anim Hosp Assoc.* 2020;56(2):59-82. doi:10.5326/jaaha-ms-7055
  168. Robertson SA, Gogolski SM, Pascoe P, Shafford HL, Sager J, Griffenhagen GM. AAFP Feline Anesthesia Guidelines. *J Feline Med Surg.* 2018;20(7):602-634. doi:10.1177/1098612X18781391
  169. Zanelli S, Buck M, Fairchild K. Physiologic and pharmacologic considerations for hypothermia therapy in neonates. *J Perinatol.* 2011;31(6):377-386. doi:10.1038/jp.2010.146
  170. Robertson S. Hypothermia - More Important Than You Believe. In: *World Small Animal Veterinary Association World Congress Proceedings.* ; 2015.
  171. Erecinska M, Thoresen M, Silver IA. Effects of hypothermia on energy metabolism in mammalian central nervous system. *J Cereb Blood Flow Metab.* 2003;23(5):513-530. doi:10.1097/01.WCB.0000066287.21705.21
  172. Steendijk P. Cardiovascular consequences of cooling in critical care. *Crit Care.* 2011;15(1):1-3. doi:10.1186/cc9989
  173. Brodeur A, Wright A, Cortes Y. Hypothermia and targeted temperature management in cats and dogs. *J Vet Emerg Crit Care.* 2017;27(2):151-163. doi:10.1111/vec.12572

174. Armstrong SR, Roberts BK, Aronsohn M. Perioperative hypothermia. *J Vet Emerg Crit Care*. 2005;15(1):32-37. doi:10.1111/j.1476-4431.2005.04033.x
175. Burton AR, Fazalbhoy A, Macefield VG. Sympathetic responses to noxious stimulation of muscle and skin. *Front Neurol*. 2016;7(JUN):1-11. doi:10.3389/fneur.2016.00109
176. Yücel MA, Aasted CM, Petkov MP, Borsook D, Boas DA, Becerra L. Specificity of Hemodynamic Brain Responses to Painful Stimuli: A functional near-infrared spectroscopy study. *Sci Rep*. 2015;5:1-9. doi:10.1038/srep09469
177. O'gara PT. The Hemodynamic Consequences of Pain and Its Management. *J Intensive Care Med*. 1988;3(1):3-5. doi:10.1177/088506668800300102